MATCHING SUPPLY TO DEMAND:

RELATING LOCAL STRUCTURAL ADAPTATION TO GLOBAL FUNCTION

A Dissertation

by

KETAKI VIMALCHANDRA DESAI

Submitted to the Office of Graduate Studies of
Texas A&M University
in partial fulfillment of the requirements for the degree of

DOCTOR OF PHILOSOPHY

May 2008

Major Subject: Biomedical Sciences

MATCHING SUPPLY TO DEMAND:

RELATING LOCAL STRUCTURAL ADAPTATION TO GLOBAL FUNCTION

A Dissertation

by

KETAKI VIMALCHANDRA DESAI

Submitted to the Office of Graduate Studies of
Texas A&M University
in partial fulfillment of the requirements for the degree of

DOCTOR OF PHILOSOPHY

Approved by:

Chair of Committee,	Christopher M. Quick
Committee Members,	Glen A. Laine
	Randolph H. Stewart
	Sarah N. Gatson
Head of Department,	Glen A. Laine

May 2008

Major Subject: Biomedical Sciences

ABSTRACT

Matching Supply to Demand: Relating Local Structural Adaptation to Global Function.

(May 2008)

Ketaki Vimalchandra Desai, B.S., Pune University

Chair of Advisory Committee: Dr. Christopher M. Quick

The heart and microvasculature have characteristics of a complex adaptive system. Extreme challenges faced by these organ systems cause structural changes which lead to global adaptation. To assess the impact of myocardial interstitial edema on the mechanical properties of the left ventricle and the myocardial interstitium, we induced acute and chronic interstitial edema in dogs. With chronic edema, the primary form of collagen changed from type I to III and left ventricular chamber compliance significantly increased. The resulting functional adaptation allows the chronically edematous heart to maintain left ventricular chamber compliance when challenged with acute edema, thus, preserving cardiac function over a wide range of interstitial fluid pressures.

To asses the effect of microvascular occlusions, we reintroduced the Pallid bat wing model and developed a novel mathematical model. We hypothesized that microvessels can switch from predominantly pressure-mediated to shear-mediated responses to ensure dilation during occlusions. Arterioles of unanesthetized Pallid bats were temporarily occluded upstream (n=8) and parallel (n=4) to vessels of interest (20-

65 μm). In both cases, the vessels of interest rapidly dilated (36±24 %, 37±33 %), illustrating that they responded appropriately to either decreased pressure or increased shear stress. The model not only reproduced this switching behavior, but reveals its origin as the nonlinear shear-pressure-radius relationship.

The properties of the heart and microvasculature were extended to characterize a "Research-Intensive Community" (RIC) model, to provide a feasible solution consistent with the Boyer Commission, to create a sustainable physiology research program. We developed and implemented the model with the aim of aligning diverse goals of participants while simultaneously optimizing research productivity. While the model radically increases the number of undergraduate students supported by a single faculty member, the inherent resilience and scalability of this complex adaptive system enables it to expand without formal institutionalization.

DEDICATION

This work is dedicated to my brother, Parimal Desai, whose untimely death made me realize the value of life. His sense of responsibility towards family and friends, and genuine fairness towards all living beings makes me strive to be a better person. You are a part of every page, every thought.

ACKNOWLEDGEMENTS

Of the many people who have been an instrumental part of my graduate education, the one person who made it all possible is my advisor, Dr. Christopher Quick. For the last five years, he has provided me unconditional support, as a professor, colleague and friend. Other than being the most intellectual person I have ever met, Dr. Quick also taught me to look at the brighter and lighter side of things. For being in the lab till the wee hours of the morning working on my papers; for endless hours of advice on matters professional as well as personal; for providing food, coffee and soda when needed; and for guiding me to achieve my goals without letting me give up, I thank you with all my heart.

I would also like to extend my heartfelt gratitude to Dr. Glen Laine, who has been more than just my committee member. His experience as a Department Head, as well as his infinite academic knowledge, provided invaluable guidance. He has been there for me whenever I needed to talk about anything in life; research, academics, ethics, science, politics, food, Harry Potter, relationships, the list is endless. I admire his never-give-up attitude as well as his ability to enjoy life to the fullest. I will always look up to him as my role model.

I have been fortunate to interact on a personal level with the other members of my committee, Dr. Randolph Stewart and Dr. Sarah Gatson. I would like to thank Dr. Stewart for all his help, including free issues of The Economist. Dr. Gatson was instrumental in providing valuable advice ranging from educational theories to interview

attire. I would like to extend a special thanks to Dr. Heaps and Dr. Wasser for career-related guidance and shelter, respectively. Yvonne Kovar and Cathy Green were always there for administrative assistance and a friendly chat.

Every graduate student develops a special relationship with other graduate students who share lab space, as well as daily afflictions and woes. For valuable suggestions and criticisms, I would like to thank my colleagues Arun Venugopal, Waqar Mohiuddin, Ranjeet Dongaonkar, Josh Meisner and Phuc Nguyen. I would like to specially thank Arun, my closest friend, for providing immense love and all the support that I could ever ask for. His genuine criticisms, affectionate chidings, and unreserved advice motivated me to work as diligently as I could. I would also like to thank my undergraduate students, especially Caleb Pettit, Bryan Sowers, Sunil Aradhya and Saniya Ali, for help with the research.

In addition to my peers, I have been fortunate to have endless help from my friends in College Station. I would like to thank Raajit Lall for being my pillar of support, through times good as well as bad. For dealing with my temper tantrums, for taking care of me when I was sick, for getting me my Aggie Ring, for driving endless miles from Austin, for chats about life, the universe and everything, I shall remain forever grateful. I would also like to thank Parchure Kaka, Samarth Patwardhan, Dr. Manasi Kelkar and Sunita Aunty for helping me in times of need. I would like to specially thank my close friends, Farukh, Nadya, Po, Mani, Aditi, Pranaya, Kaustubh, Bharati, Sarun, Rahul and Aaditya, for all their help, love and support.

Most of all I would like to thank my family, without whom none of this would have ever been possible. My mother, Jayashree Desai, taught me everything I know about life while giving me the freedom to make my own decisions. She struggled to provide me the education that I dreamed of without ever losing faith in my abilities. My father, Vimalchandra Desai, taught me to dream big and he always believed that I could achieve everything I wished for. Both my mom and dad provided the unconditional love that helped me realize my academic goals. Finally, I would like to thank Papa, Mummy, Kunashi, Shonu-tai, Uday-mama and Uncle for immense love and support.

"When you want something - the universe conspires in helping you to achieve it."

-- Paulo Coelho, The Alchemist

TABLE OF CONTENTS

Page

CHAPTER I

INTRODUCTION

Myocardial interstitial edema forms as a result of several disease states and clinical interventions. Acute myocardial interstitial edema is associated with compromised systolic and diastolic cardiac function, and increased stiffness of the left ventricular chamber. Formation of chronic myocardial interstitial edema results in deposition of interstitial collagen which causes interstitial fibrosis. To assess the impact of myocardial interstitial edema on the mechanical properties of the left ventricle and the myocardial interstitium, we induced acute and chronic interstitial edema in dogs. Acute myocardial edema was generated by coronary sinus pressure elevation while chronic myocardial edema was generated by chronic pulmonary artery banding. The pressure-volume relationships of the left ventricular myocardial interstitium and left ventricular chamber for control animals were compared with acutely and chronically edematous animals. Collagen content of non-edematous and chronically edematous animals was also compared.

In vitro experiments have established that endothelial shear-mediated responses cause dilation of blood vessels secondary to increase in blood flow and pressure-mediated responses cause vasodilation with decreased transmural pressure.

This dissertation follows the style of the *American Journal of Physiology Heart and Circulatory Physiology*.

Because it is not possible to experimentally separate these responses in an intact vascular network, investigators developed mathematical models to illustrate that shear- and pressure-mediated effects can work synergistically to support flow autoregulation. However, the competition between pressure- and shear-mediated responses leads to a fundamental dilemma when a part of a microvascular network is occluded. If there is an occlusion upstream of a particular vessel of interest, pressure-mediated responses would have to be dominant in order for it to dilate and decrease resistance. If there is an occlusion parallel to a particular vessel, shear-mediated responses would have to be dominant in order for it to dilate and provide collateral flow. We therefore reintroduced the Pallid bat wing model and developed a novel mathematical model to test the hypothesis that microvessels can switch from predominantly pressure-mediated to shear-mediated responses.

Although the Boyer Commission lamented the lack of research opportunities for all undergraduates at Research-Extensive Universities, it did not provide a feasible solution consistent with the mandate to maintain sustainable physiology research programs. The costs associated with one-on-one mentoring, as well as the lack of sufficient number of faculty, make it impractical. We therefore developed and implemented the “Research-Intensive Community” (RIC) model with the aim of aligning diverse goals of participants while simultaneously optimizing research productivity.

CHAPTER II

PROBLEM STATEMENT

The heart and microvasculature work together to ensure that blood supply matches metabolic demand, and represent two endpoints of the cardiovascular system. Despite obvious structural and functional differences, they share several salient features. First, the two organ systems adapt to local, mechanical stimuli with indirect global regulation. Second, their function is robust, i.e., they can withstand extreme challenges. Third, they efficiently match supply to demand.

Two pathologies exemplify the most extreme challenges to the ability of these two organ systems to ensure supply matches demand. Acute myocardial edema compromises cardiac function and thus affects the blood supply to vascular system. Acute microvascular occlusion prevents the perfusion of blood into the tissue. In both cases, adaptation to local mechanical stimuli leads to functional adaptation that maintains global function. However, the mechanisms relating local adaptation to changes in global function in both cases remain unknown. Two possibilities why advances have not yet been made can be identified.

First, global function of both the heart and the microvasculature are emergent properties, and reductive approaches to studying them do not elucidate a simple relationship between supply and demand. In fact, both heart and vessels have aspects of complex adaptive systems in that they are 1) composed of interacting adaptive units 2) resilient when perturbed 3) emergent and 4) inherently self organizing with minimal

expenditure of energy. However, they have not been characterized as complex adaptive systems. Second, there are very few people trained in interdisciplinary cardiovascular sciences. Research training programs, based on the 1-on-1 "research apprenticeship" model, have failed to ensure that 1) adapts to the specific sets of incentives and constraints of different departments, 2) is sustainable with minimal input of resources, and 3) can efficiently match research opportunities to demand for undergraduate research training. In this case, the underlying problem is that research programs are not complex adaptive systems: they are not 1) composed of interacting adaptive units 2) resilient when perturbed 3) emergent and 4) inherently self organizing with minimal expenditure of energy. Only recently has a model been developed that may have the characteristics to fulfill these criteria with team based RIC model, but the relationship of local team structure to global program function has not been elucidated.

The purpose of this dissertation is to explain how the heart adapts structure to successfully maintain function with edema; vessels adapt structurally to successfully maintain function with occlusion; and to apply the principles learned from these complex adaptive systems to suggest ways to design the RIC structure as a functional institutional program that is globally sustainable.

CHAPTER III

MECHANICS OF THE MYOCARDIAL INTERSTITIUM

INTRODUCTION

Myocardial interstitial edema can develop as a result of several clinical conditions such as acute and chronic arterial hypertension, acute and chronic pulmonary hypertension, acute coronary sinus hypertension; and interventions such as cardiopulmonary bypass and cardiac transplantation (29, 30, 78, 79, 83, 85, 100, 101, 117). Edema develops in the left ventricle following elevation of right-sided heart pressures as a result of elevation of coronary venous and coronary microvascular pressures and, thus, increased microvascular filtration into the myocardial interstitium (87, 117). Acute myocardial edema is associated with increased stiffness of papillary muscle (37) and impairment of left ventricular systolic and diastolic function, including decreased left ventricular chamber compliance (30, 45, 85, 117, 134).

Models of chronic myocardial edema have been shown to induce development of myocardial interstitial fibrosis (85). Formation of left ventricular edema, after two months of pulmonary artery banding in dogs, results in significantly increased interstitial collagen deposition in the myocardium of the left ventricular freewall (85). Chronic pulmonary artery banding in rats results in biventricular myocardial edema formation and increased myocardial mRNA levels of collagen types I and III within the left and right ventricular myocardium (29).

Interstitial fibrosis, developed in volume-overloaded and pressure-overloaded hearts (29, 85, 141, 142), is characterized by deposition of primarily type I collagen. This deposition results in diastolic dysfunction as observed by increased myocardial stiffness (38, 65), diminished ventricular chamber compliance (15) and slowing of ventricular relaxation (142). Collagen degradation and turnover (89, 97) as well as changes in collagen cross-linking (5, 112) could also have an impact on the physical properties of collagen and thus the myocardial interstitial matrix. However, the impact of myocardial interstitial fibrosis on ventricular mechanical properties appears to depend on the type of collagen deposited. A study comparing rats with experimental arterial hypertension to chronically-exercised rats showed evidence that a higher collagen III to collagen I ratio in the myocardium correlated with more rapid diastolic relaxation (16). How ventricular mechanical properties are affected by the type of collagen deposited during edema-induced interstitial fibrosis is not well described.

We therefore measured the end-diastolic pressure-volume relationship of both the left ventricular chamber and the left ventricular myocardial interstitium before and after acute edemagenic challenge in control animals and animals with chronically edematous hearts.

METHODS

Chronic Experimental Preparations

All procedures were approved by the Animal Welfare Committee at the University of Texas Medical School, Houston. Twenty six dogs of either sex with body

weight greater than 15 kg were used. Animals were anesthetized with 25 mg/kg thiopental sodium intravenously and intubated. Anesthesia was maintained with 0.5-1.5% halothane. Dogs were artificially ventilated with a respirator (Harvard apparatus, South Natick, Mass.) set to deliver room air at a volume of 25 ml/kg and a rate appropriate to maintain $PaCO_2$ between 35 and 40 mmHg. All animals were allowed to recuperate for a period of two months following surgery. Postoperative antibiotics and analgesics were administered by veterinarians as clinically indicated.

Intramyocardial capsules. Under sterile conditions the chest was opened through a left lateral thoracotomy exposing the heart. The pericardium was opened exposing the left ventricular myocardium. Consistent with previous studies (87), solid-state pressure transducers (Millar, Houston), encapsulated in porous polyethylene of 35 micron pore diameters, were inserted into the mid-myocardium of the left ventricle through blunt dissection. The final dimensions of the intramyocardial capsules were approximately 2x3 mm. The right ventricular myocardium is too thin to implant our solid state microtransducers and thus the right ventricular pressure-volume relationship cannot be determined utilizing this technology. To facilitate the measurement of myocardial interstitial fluid pressure, three capsules were placed in each left ventricular myocardium ensuring that at least one of the transducers would be operational two months following implantation for use in the acute protocols. Consistent with previous studies (87), the pericardium was not surgically reapproximated. Solid-state pressure transducers were used in place of fluid filled catheters in order to obtain higher fidelity (rise time less than 20 ms) recordings of myocardial interstitial hydrostatic pressure due to the constantly

changing interstitial pressures associated with myocardial contraction (87). Myocardial interstitial fluid pressure varies as a function of myocardial contraction, reaching a minimum during diastole. As a result, maximum left ventricular transmicrovascular fluid flow occurs during diastole. We therefore expressed our results in terms of myocardial interstitial fluid pressure and volume recordings obtained at end-diastole (87). Catheters from the solid-state pressure transducers were exteriorized through the thoracotomy and coiled into a subcutaneous pouch. The chest was closed with a multiple layer technique and animals were allowed to recuperate. A total of 18 animals were instrumented with interstitial fluid pressure monitoring capsules.

Pulmonary artery banding. In 11 animals, pulmonary arterial pressure was elevated by pulmonary artery banding to create chronic myocardial edema. Copper wire was encased in polyethylene tubing, to minimize erosion and scarring, and then placed around the pulmonary artery during the sterile surgical preparation. Unlike studies where the pulmonary artery was progressively occluded to mimic a model of progressive pulmonary artery stenosis (12), we banded the pulmonary artery to maintain a fixed reduction in diameter and a fixed mean pulmonary artery pressure of between 30 and 40 mmHg (28, 114, 147). With chronic body fluid redistribution pulmonary artery pressure tended to decrease over time although was sufficiently elevated in all animals to produce the desired level of myocardial edema accumulation. An increase in pulmonary artery pressure results in an increase in pressure within the thebesian veins and coronary sinus. This elevates microvascular pressure within the left ventricle, thus potentiating left ventricular myocardial edema. Elevation of right-sided circulatory pressures and

superior vena caval pressure in this model also reduces the volume of cardiac lymph that can flow into the central venous circulation, thus further potentiating myocardial edema (86). This model produces right-sided pressures within the heart and vasculature analogous to those seen in right heart failure or cor pulmonale (86). The chest was closed as indicated above and animals were allowed to recuperate for a period of two months.

Acute Experimental Preparations

Animals were anesthetized, intubated and ventilated as described in our chronic surgical preparation. Vascular lines were placed to constantly monitor arterial and venous pressures. The myocardium was exposed through a left thoracotomy as previously described.

Coronary sinus pressure elevation. A pressure monitoring Swan-Ganz balloon tipped catheter (Edwards Laboratories, Santa Ana, CA) was inserted through the right jugular vein and directed into the right atrium. The catheter was then advanced into the coronary sinus and sutured to the external wall of the sinus in such a manner as to not occlude the vessel. Mean pressure within the coronary sinus was recorded from the Swan-Ganz catheter. When the Swan-Ganz catheter balloon was inflated, graded elevations in coronary sinus pressure could be obtained. The affixing suture ensured that the balloon could not be ejected from the coronary sinus. With coronary sinus pressure elevation, microvascular pressure within the myocardium increases, potentiating the rate at which fluid enters the myocardial interstitium. Coronary sinus pressure was thus

elevated in a stepwise fashion in control dogs and in those with chronic myocardial edema to potentiate edema formation and compromise cardiac function (87).

Left ventricular myocardial interstitial fluid pressure. The chronically implanted Millar catheters were exteriorized from their skin pouch and connected to Millar amplifiers (Millar, Houston) and recorders. Viewed microscopically, the porous polyethylene capsules were found to be encased in loose connective tissue surrounded by normal myocyctes with no visible signs of inflammation or scarring. Each catheter was tested to determine the reliability of its myocardial interstitial fluid pressure measurements. Compression of the tissue over the catheters produced a high fidelity change in myocardial interstitial fluid pressure. A second test occasionally used was acutely changing the circulating colloid osmotic pressure either through hemodilution or colloid administration. All these interventions manifest themselves through changes in myocardial interstitial fluid pressure. Any catheter not responding appropriately was not utilized (88). Since myocardial interstitial fluid pressure can be impacted by external or internal compression, myocardial left ventricular interstitial fluid pressure at end-diastole (P_{INT}) was normalized. This normalized value was expressed as P_{INT} minus left ventricular end-diastolic chamber pressure. Except during left ventricular volume infusion to determine left ventricular chamber compliance, the baseline left ventricular end-diastolic chamber pressure was not elevated in our chronic preparation and did not change during the course of our experiments.

Left ventricular chamber compliance. Left ventricular volume was determined by inserting an Edwards impedance catheter (Santa Ana, CA) through the aorta into the left

ventricular chamber. A Millar solid-state pressure transducer was also introduced into the left ventricle to measure left ventricular end-diastolic chamber pressure along with a catheter for volume infusion. We then infused isotonic saline directly into the left ventricle at a rate that increased left ventricular end-diastolic chamber pressure by 7 to 8 mmHg in each animal. Unlike intravenous volume transfusion, right-sided vascular pressures (coronary sinus pressure) did not change during volume infusion. After maintaining a stable elevated left ventricular end-diastolic chamber pressure for 5 minutes, left ventricular end-diastolic chamber volume was again determined three times. Because compliance varies with the location on the ventricular pressure-volume curve, we calculated the left ventricular chamber compliance as the change in left ventricular end-diastolic chamber volume (ΔEDV) divided by the change in left ventricular end-diastolic chamber pressure (ΔEDP).

$$\text{Left Ventricular Chamber Compliance} = \frac{\Delta EDV}{\Delta EDP} = \frac{EDV_2 - EDV_1}{EDP_2 - EDP_1} \qquad (3.1)$$

where, EDV_1 is the initial left ventricular end-diastolic chamber volume, EDP_1 is the initial left ventricular end-diastolic chamber pressure, EDV_2 is the left ventricular end-diastolic chamber volume after saline infusion, and EDP_2 is the left ventricular end-diastolic chamber pressure after saline infusion. At the conclusion of each protocol, animals were euthanized with an overdose of thiopental sodium and 20 ml saturated potassium chloride solution.

Wet to dry weight ratio (myocardial edema). The amount of myocardial edema or extravascular fluid (EVF) was obtained from the ***unitless*** blood free (wet weight - dry weight)/dry weight ratio for the left ventricular myocardium. Following removal of tissue for collagen digestion and histological analysis of porous polyethylene capsules, the myocardium was homogenized. A spectrophotometric correction for blood volume was performed since the volume of blood and consequently water found within the coronary vasculature may vary throughout the course of an experiment (84). The homogenate was then weighed and dried to a constant weight. We have previously demonstrated that this procedure quantifies extracellular, extravascular fluid volume changes or myocardial interstitial edema since cellular volume remains constant (85). Control myocardial extravascular fluid values obtained during the left ventricular chamber compliance protocol were determined by transmural myocardial biopsy (once in control animals prior to generating acute edema), following which cardiac tissue was placed in a (kerosene/bromobenzene) gradient column to determine percent water and extravascular fluid (50, 85). The myocardial interstitial pressure-volume relationship was expressed as extravascular fluid i.e. myocardial edema plotted against normalized left ventricular end-diastolic interstitial fluid pressure.

Collagen analysis. Total myocardial fibrosis can be estimated by the amount of collagen in the myocardial interstitium. Hydroxyprolene concentration within the myocardium was determined using the method described by Weber et al. (142) and confirmed with an amino acid analyzer. Since collagen contains approximately 13.4% hydroxyprolene (85, 142), the collagen content of the specimen was calculated by

multiplying the hydroxyprolene content by 7.46. The concentration of collagen was expressed as milligrams of collagen per 100 mg dry ventricular weight. Samples of left ventricular myocardium taken for collagen typing were lyophilized and pulverized. An aliquot was used for solubilization and determination for collagen types. Samples were initially extracted using 1M NaCl in 0.05M Tris buffer, pH 7.4, at 4˚C, containing protease inhibitors for 24 hours. Supernatants were separated by centrifuging and heart residue extracted in 0.5M acetic acid. Pepsin (1mg/ml) digestions were performed three times on residues at 4˚C in 0.5M acetic acid for 24 hours. The three pepsin extracts were pooled for collagen precipitation, which was collected by centrifugation (7, 68). The relative percentage of collagen types I and III was determined through SDS gel electrophoresis (137, 142). Following scanning of stained gels with a densitometer, the quantities of collagen types I and III were determined by planimetry (137).

Experimental Groups

Protocol 1: Determining the effect of chronic myocardial edema on the left ventricular myocardial interstitial pressure-volume relationship

Group 1a. To determine the pressure-volume relationship for the left ventricular myocardial interstitium, baseline data for left ventricular end-diastolic interstitial fluid pressure (chronically implanted porous polyethylene capsules) and myocardial extravascular fluid [(wet weight - dry weight) / dry weight] were obtained from two animals. These data were compared to 48 historic controls from our laboratory. Since the new control values were not different from existing controls, data were pooled (85). In eight additional animals, left ventricular end-diastolic interstitial fluid pressure and

myocardial extravascular fluid were determined after edema was acutely formed by coronary sinus pressure elevation.

Group 1b. Left ventricular myocardial interstitial fluid pressure at end-diastole and myocardial extravascular fluid were determined in eight animals with chronic myocardial edema resulting from chronic pulmonary artery banding. Acute myocardial edema was generated by acute coronary sinus pressure elevation in five of these animals. This group was designed to simulate patients with chronic right heart failure or pulmonary disease, which elevates right-sided circulatory pressures thus potentiating myocardial edema (86).

Protocol 2: Determining the effect of chronic myocardial edema on left ventricular chamber compliance

Group 2a. In five animals, left ventricular chamber compliance was calculated after left ventricular myocardial edema formation was potentiated by coronary sinus pressure elevation.

Group 2b. In three animals with chronic myocardial edema secondary to pulmonary artery banding, left ventricular chamber compliance was determined at baseline and following additional acute myocardial edema formation.

Statistical Analysis

All data are presented as the mean $\pm$ standard error of the mean (SEM). Normalized left ventricular end-diastolic interstitial fluid pressures and myocardial extravascular fluid values were compared using either a student's *t*-test or a paired *t*-test. A p value less than 0.05 was considered significant. Regression equations were

calculated using the least squares method (109). The co-efficients of the regression equations representing the slopes and y-axis intercepts were compared using Student's *t*-test (109).

RESULTS

Table 3-1 summarizes the experimental interventions performed in each group along with the measured parameters. In brief, subjects in groups 1a and 2a did not have pulmonary artery banding and chronic myocardial edema. The 1a group was used as baseline, and left ventricular end-diastolic interstitial fluid pressure and myocardial extravascular fluid were measured. In the 1a control group, left ventricular end-diastolic interstitial fluid pressure and myocardial extravascular fluid were measured before and following acute myocardial edema formation. Left ventricular chamber compliance was calculated for group 2a prior to elevation of coronary sinus pressure. It was calculated again following the generation of acute myocardial edema. Subjects in groups 1b and 2b had their pulmonary artery banded to induce chronic myocardial edema. Left ventricular end-diastolic interstitial fluid pressure and myocardial extravascular fluid were measured for group 1b, and left ventricular chamber compliance was calculated for group 2b. Additional acute myocardial edema was then generated in all chronically edematous animals, with the exception of control animals with chronic edema, and all measurements were repeated.

Normalized values of left ventricular end-diastolic interstitial fluid pressure as a function of myocardial extravascular fluid are illustrated in Fig. 3-1. In control animals

(Group 1a: baseline, n=50), at a baseline myocardial extravascular fluid value of 2.9±0.07 [(wet weight-dry weight)/dry weight], normalized left ventricular end-diastolic interstitial fluid pressure was 14.9±1.1 mmHg. Elevating coronary sinus pressure resulted in the formation of acute myocardial edema (Group 1a: control animals, n=8), that manifests itself as an increase in myocardial extravascular fluid volume. As the EVF changed from baseline to 3.5±0.03 (p<0.01), normalized left ventricular end-diastolic interstitial fluid pressure changed from 14.9±1.1 to 37.5±1.8 mmHg (p<0.01). The baseline value for myocardial extravascular fluid for subjects with chronic edema (Group 1b: control animals, n=3) was significantly higher than the myocardial EVF value of subjects in group 1a: baseline. We compared the normalized values of left ventricular interstitial fluid pressure at end-diastole in control animals with acute edema (37.5±1.8 mmHg) to animals with chronic edema (22.2±1.4 mmHg) (Group 1b: chronically edematous, n=5). At a myocardial extravascular fluid value of 3.5±0.03, normalized left ventricular interstitial end-diastolic pressures in the two sets of animals were significantly different (p<0.01). Generation of acute edema in chronically edematous subjects also increased the normalized left ventricular end-diastolic interstitial fluid pressure values from 22.2±1.4 mmHg at control to 45±2.4 mmHg (p<0.01) at an EVF of 3.6±0.04. It is interesting to note that further increasing myocardial extravascular fluid above 3.5 did not increase normalized left ventricular end-diastolic interstitial fluid pressure in animals with chronically edematous hearts.

Figure 3-2 demonstrates left ventricular chamber compliance plotted as a function of myocardial extravascular fluid (EVF). Regression lines were plotted for

control data (y=-4.11x+15.64, r^2=0.67) and chronic myocardial edema data (y=-4.70x+20.73, r^2=0.86). In control animals (Group 2a: control animals, n=5), the negative slope of the regression line demonstrates that left ventricular chamber compliance decreased in animals made acutely edematous, indicating that hearts became stiffer. Animals with chronic edema (Group 2b: chronically edematous, n=3), following pulmonary artery banding, also demonstrated a decrease in left ventricular chamber compliance when they were made acutely edematous, also indicated by the negative slope of the regression line. The slopes of the control regression line and the chronic edema regression line could not be shown to be significantly different (109). Before generation of acute edema, left ventricular chamber compliance was higher in chronically edematous animals when compared to non-edematous animals.

Myocardial collagen content in the control group 1a was 3.9$\pm$0.44 mg/100 mg dry wt. and 5.8$\pm$0.34 mg/100 mg dry wt. in the chronic edema group 1b, demonstrating a significant difference. The distribution of left ventricular collagen changed when animals were made chronically edematous; the percentage of type III collagen increased from 11% in control animals to approximately 90% in animals with chronic edema, while the percentage of type I collagen decreased from 85% to approximately 10%.

Figure 3-3 illustrates left ventricular chamber compliance as a function of the normalized left ventricular end-diastolic interstitial fluid pressure. Left ventricular chamber compliance values were obtained by substituting myocardial extravascular fluid values from Fig. 3-1 into regression equations from Fig. 3-2. Standard deviations for left ventricular chamber compliance were also computed from regression equations from

Fig. 3-2. We placed boundary limits on the lower values of myocardial EVF to avoid negative or non-physiologic values for left ventricular chamber compliance (see Fig. 3-3). Left ventricular chamber compliance was lower in acutely edematous animals (1.24 mL/mmHg) at normalized left ventricular end-diastolic interstitial fluid pressure value of 37.5$\pm$1.8 mmHg, when compared to non-edematous control animals (3.71 mL/mmHg) at 14.9$\pm$1.1 mmHg. Animals with chronic edema demonstrated a higher control value of left ventricular chamber compliance (4.27 mL/mmHg) when compared to non-edematous control animals (3.71 mL/mmHg). Even after acutely elevating left ventricular end-diastolic interstitial pressure in chronically edematous animals to 45 mmHg, the left ventricular chamber compliance value remained relatively high at 3.8 mL/mmHg. As illustrated in Fig. 3-3, the points representing animals with chronic edema are shifted to the right, indicating a more compliant myocardium at any given left ventricular end-diastolic interstitial fluid pressure.

DISCUSSION

Generating acute edema in both control and chronic animals resulted in increased stiffness of the left ventricular chamber. Chronically edematous hearts had higher left ventricular chamber compliance when compared to non-edematous control hearts (Fig. 3-2). Compared to control animals, the percentage of type III collagen in the left ventricles of chronically edematous hearts was significantly higher, and type I collagen was significantly lower.

This study is the first to characterize the pressure-volume relationship of the left ventricular myocardial interstitium subjected to acute and chronic edema. Animals subjected to an acute increase in myocardial extravascular fluid or myocardial edema exhibit an increase in stiffness of their left ventricular myocardial interstitium. However, when animals with chronic myocardial edema were subjected to acute edemagenic conditions, their pressure-volume relationships demonstrated a right shift in the curve when compared to control animals with acute edema (Fig. 3-1). In other words, generating acute myocardial interstitial edema in control animals resulted in an increase in left ventricular end-diastolic interstitial fluid pressure, which was significantly higher than that resulting from a comparable increase in myocardial extravascular fluid in animals with chronic edema. The pressure-volume relationships were plotted by joining data points linearly and not as regression lines (Fig. 3-1). If the curves were plotted non-linearly, there would still be a right shift for animals with chronic myocardial edema. We were confident that increasing myocardial extravascular fluid to approximately 3.5 [(wet weight-dry weight)/dry weight] would raise myocardial left ventricular end-diastolic interstitial fluid pressures. However, additional increase in myocardial extravascular fluid did not raise left ventricular end-diastolic interstitial fluid pressure beyond approximately 50 mmHg in either acute or chronic conditions. We speculate that damage to the interstitial matrix (which may or may not be reversible) may have occurred. We anticipated that the curve would break in the opposite direction resulting in significantly elevated interstitial pressures for relatively small increases in volume. We believe that when capillary pressure increases to approximately 50 mmHg following coronary sinus

pressure elevation, there is enhanced venous outflow from the thebesian veins (62, 64) into the right ventricle where the pressure is relatively lower. Opening of the lower resistance thebesian outflow limits the elevation in myocardial microvascular pressure, and thus left ventricular end-diastolic interstitial fluid pressure, from exceeding approximately 50 mmHg. An alternate explanation is that the heart may attempt to decrease interstitial pressure by shunting fluid across the myocardial surface (transudation). This would keep interstitial pressure at a lower level and eliminate the potential for microvascular collapse and cardiac death. Another explanation is that the myocardium is not homogeneous and, at higher pressures, fluid may be accumulating in places other than where the transducers were recording pressures.

Acutely elevating the myocardial interstitial fluid content of the left ventricular interstitium resulted in decreased compliance of the left ventricular chamber in both non-edematous control and chronically edematous animals. We hypothesized that left ventricular chamber compliance would be lower and the left ventricle would be stiffer in chronically edematous animals under control conditions. However, chamber compliance of hearts with chronic myocardial edema was higher under control conditions when compared to non-edematous hearts. The information presented in Fig. 3-3 was derived from the data in Fig. 3-1 substituted into the regression equations of Fig. 3-2, determined using the methods of least squares. Because this does not always result in a perfect fit (as indicated by the r squared values), it was possible for slightly negative values for compliance to be computed. This concept is called to the reader's attention, since

negative compliance values have no physiologic meaning and simply represent a statistical anomaly.

The quantity of interstitial fibrosis in the heart can be estimated by the amount of collagen in the myocardial interstitium. Myocardial collagen is comprised primarily of types I, III and V, with type I collagen predominating (65). Characteristics of the type of collagen play a marked role in determining the behavior of the myocardial interstitium. While type I collagen is composed of larger diameter fibers with greater stiffness, type III collagen is relatively more distensible with small diameter fibers (15, 65). Since fibrillar type I collagen is relatively stiff, small changes in its content can impact functional properties of the heart. It has been hypothesized that the increased collagen content, and not left ventricular mass, during systemic hypertension results in diastolic dysfunction (15, 66). This could be attributed to an increase in the collagen type I to type III ratio, which could be responsible for the increased stiffness of the left ventricle (146). Increased collagen deposition in the heart can be attributed to increased collagen expression in response to variations in hemodynamic loading (18). Depending on the heart's response to these mechanical stimuli, cardiac fibroblasts may activate different signal transduction pathways to regulate the fibrotic content of the myocardium (3). Thus, hypertensive hearts responded to pressure-overload resulting in increased collagen type I concentration and a stiffer myocardium. Type I collagen fibrosis predominates in the left ventricular myocardium exposed to an increased afterload. The right ventricle also hypertrophies when challenged by an elevated vascular outflow pressure (pulmonary artery pressure) (114) similar to how the left ventricle responds to systemic

arterial hypertension (38). We speculate that in a model of pulmonary artery hypertension, the right ventricle, exposed to pressure overload, would have an elevated collagen type I/type III ratio. We did not perform analysis of the right ventricle in our study due to physical constraints in implanting the porous polyethylene capsules. However, it would be interesting to know if right ventricular fibrosis with type I collagen takes place in our model of pulmonary artery hypertension (increased right ventricular afterload). When our animals were made chronically edematous (with no pressure-overload), type I collagen was replaced by type III collagen. Because collagen has a rapid turnover (89, 97), it would be unlikely to observe any transient changes in the type after 2 months. Increased distensible type III collagen may be responsible for the increased left ventricular chamber compliance in chronically edematous hearts. We have previously demonstrated a similar increase in compliance and interstitial distensibility or decreased stiffness of the small bowel in conjunction with gastrointestinal edema (124, 126). The concept of 'compliance resetting' in chronic disease has also been addressed in the bioengineering literature (42, 43, 46).

Banding of the pulmonary artery and generation of chronic myocardial interstitial edema resulted in structural adaptation of the left ventricle. Although we did not conduct any studies to characterize a causal relationship between changes in collagen degradation or cross-linking and adaptive remodeling of the heart, we did observe a shift in the primary collagen type in the left ventricle from type I to III. For a given left ventricular end-diastolic interstitial fluid pressure (Fig. 3-3), chronically edematous hearts had higher left ventricular chamber compliance when compared to non-edematous or acutely

edematous hearts. We believe that patients with chronically edematous hearts are better equipped to cope with certain pathological conditions (30, 83, 85, 100, 101, 117) associated with acute edema formation compared to patients with non-edematous hearts. This change in left ventricular chamber compliance could be attributed to the distensible fibers of collagen type III that were laid down during the development of chronic myocardial edema in these animals. The concept of adaptive remodeling of the interstitium to regulate compliance has been previously demonstrated in several models (42, 43, 46, 78, 79, 124-126).

Adaptive remodeling of the chronically edematous myocardial interstitium could result from factors other than a shift in predominant collagen type. In order to assess structural changes in the myocardial interstitial matrix, collagen biochemistry including studies of concentration, types, ratios, turnover and degradation (89, 97) as well as changes in cross-linking (5, 112), would be valuable. Our protocols were designed primarily to evaluate myocardial interstitial matrix mechanics. A future study could be designed to evaluate collagen biochemistry and histology of not only the left ventricle, which could provide an alternative explanation for the shift in myocardial interstitial pressure-volume relationship, but also of the right ventricle, which has not been adequately characterized. Samples of the right and left ventricle could be taken on a daily or weekly basis, because of the rapid rate of collagen degradation and turnover (89, 97), during the development of myocardial edema and interstitial fibrosis. However, due to high costs associated with chronic canine studies and the significant numbers required to track biochemical changes over shorter time intervals (to detect changes in

degradation and cross-linking), a rat model may be more appropriate. Such studies would, however, preclude evaluation of interstitial mechanics.

CHAPTER IV

SHEAR-MYOGENIC SWITCH

INTRODUCTION

Although the buildup of metabolites such as adenosine, potassium, and acetylcholine plays a fundamental role when blood supply does not meet tissue demand (56), it is insufficient to explain flow autoregulation. Because metabolite-driven arterial dilation has a slow response time (22, 145) and has minimal effects on upstream vessels (8, 80), investigators began to explore two local mechanical stimuli—transmural pressure (8, 32) and endothelial shear stress (53, 75, 76). The pressure-mediated myogenic response is endothelium independent, and is characterized by constriction of blood vessels when transmural pressure increases and dilation when transmural pressure decreases (128). A decrease in perfusion pressure causes a myogenic dilation in vessels within seconds, thus, lowering vascular resistance and partially restoring blood flow. On the other hand, the shear-mediated response is endothelium-dependent, and is characterized by a dilation of vessels when flow increases, and a constriction when flow decreases (70, 82). When tissue metabolic rate increases and local resistance arterioles dilate, the increased flow causes a secondary dilation of feeding arterioles, augmenting flow. These pressure- and shear-mediated responses therefore act synergistically to aid flow autoregulation (71).

Pressure-mediated and shear-mediated responses compete when shear stress and transmural pressure either simultaneously increase or simultaneously decrease (81). In

either case, there is no governing principle predicting whether the competing responses result in vasodilation or vasoconstriction. The apparent dominance of the pressure-mediated response over the shear-mediated response has been demonstrated in a number of systems including rabbit cerebral arteries (139), pig coronary arterioles (81) and rat skeletal muscle arterioles (135). Investigators have also shown that increases in pressure elicits a myogenic constriction, even if accompanied by increased metabolites and reduced oxygen tension (102). In stark contrast, the dominance of the shear-mediated response over the pressure-mediated response has been demonstrated in small rabbit conductance arteries (36, 54, 72, 116). The conflicting reports have been particularly difficult to reconcile because each intervention affects pressure and shear differently (19), and each vessel has different sensitivities to changes in pressure and shear (34, 52, 82).

Although occlusion of arterioles in a microvascular network can occur with micro emboli (149), fat emboli (4), or platelet aggregation (136), it has been studied far less than occlusion of large conductance vessels. Unlike conductance vessels in organ systems with well-defined collateral vessels (127), the resistance arterioles can act as a plexus, have numerous arcuate arterioles interconnecting branches, and even exhibit circular arcade structures (31, 35). Thus, there are multiple pathways for blood to re-establish flow, and any arteriole could act as a collateral. Occlusion upstream of a particular arteriole causes a simultaneous decrease in shear stress and pressure (69), therefore causing shear- and pressure-mediated responses to compete. Ameliorating the resulting compromised perfusion would require a dominant pressure-mediated response.

However, occlusion parallel to the same arteriole causes a simultaneous increase in shear stress and pressure (99), also causing shear- and pressure-mediated responses to compete. However, ameliorating the resulting compromised perfusion would require a dominant shear-mediated response. It has yet to be determined how arterioles can selectively switch from pressure-dominated responses to shear-dominated responses.

The behavior of blood vessels differ significantly depending on whether they are studied in vitro, in situ or in vivo (148). Although in vitro studies were able to demonstrate pressure- and shear-mediated responses in a single vessel (34, 77), they cannot address how transmural pressure and endothelial shear stress co-vary in a vascular network. Studies conducted in situ incorporate metabolic factors, but the inability to experimentally abolish the pressure-mediated response makes it difficult to determine differential responses to changes in metabolites, shear stress and transmural pressure. Potential dilatory effects of anesthesia (129), inflammation secondary to surgical trauma (148), and conducted stimuli from nearby vessels (40, 41), can limit the ability to interpret the results of in vivo experiments. The batwing model has been critical to our current understanding of the myogenic effect in vivo, because it allowed the noninvasive characterization of the vasculature to changes in pressure (31, 33). However, it fell out of use before shear-mediated dilation was fully appreciated. The lack of conventional animal models amenable to noninvasive experimentation and the inability to completely block the individual effects of metabolites, shear- and pressure-mediated responses led to the development of mathematical models (26, 47, 122, 123, 140).

Pries et al. (31, 120-122) developed a series of large-scale mathematical models that captured the complex interaction of four stimuli of chronic vascular adaptation. Although these models have been critical for understanding the emergent properties of vascular networks (119), their complexity makes it difficult to ascribe network behavior to any specific mechanism. By taking a simpler approach that eliminated two stimuli, Quick et al. (123) revealed that observed shifts in the lower level of autoregulation can be ascribed to pressure-mediated arterial dilation. Another approach first modeled arterial beds as single vessel with a pressure-mediated response (27), then two vessels with shear- and pressure-mediated responses (58), and, finally, a symmetrical bifurcating network with each vessel exhibiting metabolite-, pressure-, and shear-mediated responses (92). Capturing ever-increasing levels of complexity, investigators have successfully modeled coronary (26), cerebral (140), renal (113), and skeletal (13) networks. In particular, the model developed by Liao et al. (92) illustrated how heterogeneity in the sensitivity of the shear-and pressure-mediated responses aided normal autoregulation. Integral to their model was an assumption of a symmetrical tree structure without interconnections that could act as collaterals in the event of regional occlusion. Because this model incorporated realistic interaction of pressure- and shear-mediated responses, the results of microvascular occlusions can be addressed with only a minor increase in complexity.

In summary, although pressure- and shear-mediated responses act together to aid flow autoregulation, reconciling the conflicting reports when these responses compete and explaining how they interact to ameliorate compromised perfusion cannot be

accomplished with conventional animal or mathematical models. We therefore developed a simple mathematical model and re-introduced the classic Pallid bat wing model to do so.

Theory

Hemodynamics of a single vessel. The radius (r) of a vessel determines its vascular resistance (R), which in turn determines the amount of blood flowing through the vessel and the axial pressure gradient across it (123). The resistance of an arteriole can be approximated from Poiseuille's law,

$$R(r) = \frac{\Delta P}{Q} = \frac{8\eta L}{\pi r^4} \qquad (4.1)$$

where ΔP is the axial pressure gradient, Q is the blood flow, η is viscosity of blood and L is arteriolar length. Radius also determines the endothelial shear stress (τ), the frictional force acting on the endothelium due to the flow of blood. Endothelial shear stress can be expressed in terms of Q, or alternatively mean blood velocity (v),

$$\tau = \frac{4\eta Q}{\pi R^3} = 4\eta \frac{v}{r} \qquad (4.2)$$

The expression v/r is referred to as the "pseudo shear rate" (11). Endothelial shear stress was calculated for the mathematical model, while pseudo shear rate was calculated from measured r and v values for the experimental model.

Predicting pressure and shear stress in a network model. Figure 4-1 illustrates a network of arterioles represented in terms of their resistances. The network was constructed with the minimum number of arterioles necessary to achieve our goals. The upstream arteriole was designated as M_{in}, the parallel arteriole as M_p, the collateral as

M_c, and the vessel of interest as M_v. The network was asymmetric, and incorporates 1st and 2nd order arterioles, characterized by two parameters, *r* and *L*. Consistent with accepted modeling methodology (123), pressure drops across the vessels are governed by Poiseuille's Law (*Eq. 4.1*), and flows through them are governed by conservation of mass. Arteriolar network inlet pressure (P_{in}) was set at 100 cmH_2O, and the outlet capillary pressure (P_{out}) was set at 50 cmH_2O (31). Pressures at the outlet of one vessel were set equal to the pressure at the inlet of the following vessels. Pressures P_1, P_2 and P_3 denote transmural pressure at the junctions. Resistances for vessels M_{in}, M_p, M_c, M_{out} were chosen such that pressure P_1, P_2 and P_3 were consistent with published values (1, 2, 1.43, and 50 $mmHg \cdot sec \cdot nl^{-1}$, respectively)(31). The pressure of the collateral vessel (P_c) was set at the initial pressure P_2. Using the known values of diameter (31) and length (approximately 6 mm for the vessel of interest) from the bat wing vasculature, *Eqs. 4.1 and 4.2* were solved simultaneously for pressure and flow using standard methods (123).

Vessel adaptation. To simplify the model, only one arteriole in the network (circle, Fig. 4-1) was set to adapt with changes in pressure and endothelial shear stress, while all others had constant radii. In this case, adaptation of the vessel of interest (M_v) to changes in transmural pressure (myogenic response) and endothelial shear stress (shear-mediated dilation) were based on a model of coronary vessels developed by Liao et al (92). This model characterized the arterioles of the coronary microvasculature from different levels of the network. Summarizing briefly, the steady-state diameter (*D*) of an arteriole was characterized assuming

$$D = D_m + (D_p - D_m)F_\tau, \qquad (4.3)$$

where D_p was the steady-state passive diameter at transmural pressure P, D_m represented the activation of smooth muscle due to the myogenic response in the absence of flow, and F_τ represented the normalized effect of endothelial shear stress. The value of P is taken to be an average of vessel inlet and outlet pressures. The steady-state passive curve was characterized by an empirical equation,

$$D_p = D_0 + \frac{(D_{max} - D_0)(\frac{P}{P_p})}{[1 + (\frac{P}{P_p})]} \tag{4.4}$$

where P_p and D_0 are empirical parameters. Similarly, the myogenic response was characterized by an empirical equation,

$$D_m = D_{min} + \frac{(D_0 - D_{min})}{[1 + (\frac{P}{P_m})^m]} + \frac{(D_{max} - D_{min})(\frac{P}{P_p})^y}{[1 + (\frac{P}{P_y})^y]} \tag{4.5}$$

where D_{max}, P_y D_{min}, P_m, P_y, m, and y were empirical parameters. The response to shear-mediated dilation was normalized between 0 and 1 and governed by an empirical equation:

$$F_\tau = \frac{F_{max} + (\frac{\tau}{K_\tau})^s}{[1 + (\frac{\tau}{K_\tau})^s]} \tag{4.6}$$

where F_{max}, K_τ , and s were empirical parameters. The value of K_τ represented the fractional shear-mediated dilation and varied from 0 to 1. Calculated values of P and τ were substituted from the simple network model into *Eqs. 4.3-4.6* to obtain an

instantaneous value of arteriolar diameter for the vessel of interest, M_v. Parameters P_p, D_0, D_{max}, P_y D_{min}, P_m, P_y, m, y, F_{max}, K_τ, and s were assumed equal to those determined for the intermediate-sized coronary arterioles (45-108 μm diameters) used to develop the original Liao et al. model (92). The instantaneous diameter value was used to iteratively calculate new pressures and shear stresses in the vessel of interest to obtain a value for steady-state diameter.

METHODS

Mathematical Modeling Methods

Parallel and upstream occlusions. Two modeling experiments were performed to determine how a vessel of interest (M_v) was affected by occlusion of an upstream (M_{in}) and parallel (M_p) vessel (Fig. 4-1). In the first modeling experiment, an upstream arteriole (M_{in}) was progressively occluded from 0 to 100%, and the resulting steady-state pressures, shear stresses, and diameters of the vessel of interest were calculated. To simulate the change in diameter with time, diameter was allowed to change no more than 1μm/sec (31). The resulting change in radius in the vessel of interest after 100% occlusion of M_{in} was plotted as a function of time. Although the upstream arteriole was occluded, flow continued through collateral arteriole (M_c). In the second modeling experiment, the parallel arteriole (M_p) was progressively occluded from 0 to 100%, and the resulting steady-state pressures, normalized shear stresses, and diameters of the vessel of interest were calculated. The resulting change in radius in the vessel of interest after 100% occlusion of M_p was also plotted as a function of time.

Contour plots. A contour plot was used to characterize the relationship between radius, transmural pressure and normalized shear stress in the vessel of interest. The steady-state changes in transmural pressure and normalized shear stress resulting from parallel and upstream occlusions were then determined and plotted with the contour plot.

Experimental Methods

Pallid bat experimental model. Experimental procedures and animal care were performed in compliance with the Texas A&M University Institutional Animal Care and Use Committee and were similar to those reported previously (143). Experiments were conducted on 8 Pallid bats of either sex, weighing between 15-35g. Each bat was trained to be amenable to light restraint, ensuring minimal movement of the wing during the course of the experiment. They were housed in a room with constant temperature year round.

Bat restraint. Unanesthetized bats were placed in a custom box (143) and experiments were conducted at a fixed lab temperature of approximately 26^{o}C. The box allowed for free extension of the left wing, which was lightly restrained over a Plexiglas plate by cotton applicators, as described by Davis et al. (31). The box was placed under the microscope for vessel observation and data acquisition.

Data collection and acquisition system. The microscope used for the study was a fixed stage upright microscope (BX61WI, Olympus, Pennsylvania) with a water-immersion objective. The microscope image was captured by a video camera (KR222 S-Video Camera, Panasonic, New Jersey) and relayed to a computer. Magnifications of 400X were used for data acquisition. Light intensity was maintained at a level low

enough to avoid evoking vascular responses. The acquired image was recorded using custom software (Lab View 7.1, National Instruments, Texas). An Optical Doppler Velocimeter (Optical Doppler Velocimeter Model #4, A&M Health Systems, Texas) was connected between the camera and the microscope, and obtained the center-line red blood cell velocity. For diameter measurements, customized software (103) recorded the real-time changes in arteriolar diameter at 30 frames per second.

Classification of microvessels. We studied several bifurcations of a branching arteriolar tree in the wing between the fourth and fifth digits of the Pallid bat (Fig. 4-2). Measurements were made on 1^{st}-4^{th} order arterioles adjacent to bifurcations. Data were collected at bifurcations for ease of identification and for comparison across different subjects. The arterioles were named similar to those in the mathematical model (Fig. 4-1); while arterioles in the model were denoted by the letter M, those in the bat wing were denoted by the letter B.

Noninvasive acute microvascular occlusions. As illustrated in Fig 4-2, the first arteriolar bifurcation (i.e. B_{in}, B_p and B_v) and then the subsequent bifurcations were located, and real-time diameters and velocities were obtained for 3 minutes to establish baseline values. Radii and velocities were used to calculate the pseudo shear rate (*Eq. 4. 2*), because viscosity was assumed to be constant. To selectively occlude B_{in} and B_p, 100 µl glass pipettes (Borosilicate pipettes, WPI, Florida) were pulled (PUL-100, WPI, Florida) to form a sharp tip, and then blunted by heating with a Bunsen burner until the tip was approximately 30-50 µm in diameter. Pipettes were mounted on micromanipulators (MC-35A, Narishige, Japan) for precise control and positioning. On

100x magnification, the pipette was carefully lowered over target arterioles until blood flow was observed to cease.

Occlusion protocols. At each bifurcation, two experimental protocols were performed while observing the vessel of interest B_v (Fig. 4-3A). In the first protocol, only four of the total eight bats were used, to confirm consistency with previously published results (99, 133). First, the control data were obtained, and then the parallel arteriole B_p was occluded (Fig. 4-3B). The magnification was returned to 400X to obtain the arteriolar diameter and red blood cell velocity of the blood flow at B_{in}, B_p and B_v. Data were recorded after two minutes of stabilization. Once the pipette was in place, the arterioles stayed occluded for the entire duration of the data acquisition. Data were recorded for three minutes for seven arterioles. The procedure for second protocol was similar to parallel occlusions; however, the position of occlusion was moved upstream to B_{in} (Fig. 4-3C). To obtain real-time diameters and pseudo shear rate values, data were recorded continuously for 100 seconds before and during occlusion. Data were also recorded after two minutes of stabilization for twenty-five arterioles. Both procedures were analogous to the modeling methods where M_v was the vessel of interest and M_p and M_{in} were occluded. No bat was used for more than one protocol on any given day.

Statistical analysis. The difference between baseline and occluded values of pseudo shear rate and arteriolar diameter were compared using Student's t-tests, and a *p-value* of less than 0.05 was considered significant. Percentage changes in diameter and pseudo shear rate for both parallel and upstream occlusion protocols were first calculated

for 1^{st}-4^{th} order bifurcations and then averaged for all the bats. Data was represented as mean $\pm$ standard deviation.

RESULTS

Modeling Results

Figure 4-4A demonstrates the effect of 100% occlusion of the parallel arteriole M_p on the vessel of interest, M_v. Figure 4-4B demonstrates the effect of 100% occlusion of the upstream arteriole M_{in} on the vessel of interest, M_v. Once steady-state diameter was obtained, the parallel occlusion resulted in 8% dilation, and the upstream occlusion resulted in 14% dilation.

Figure 4-5 demonstrates the changes in transmural pressure, normalized endothelial shear stress and arteriolar diameter as parallel arteriole M_p is progressively occluded. Both transmural pressure and normalized endothelial shear stress increased (2% and 75%, respectively), while arteriolar diameter increased by 8%.

Figure 4-6 demonstrates the changes in transmural pressure, normalized endothelial shear stress and arteriolar diameter as upstream arteriole M_{in} is progressively occluded. Both transmural pressure and normalized endothelial shear stress decreased (47% and 97%, respectively), while arteriolar diameter increased by 14%.

Figure 4-7 illustrates a contour plot of arteriolar diameter of the vessel of interest as a function of transmural pressure and normalized endothelial shear stress. One arrow indicates that when a parallel arteriole was occluded, both transmural pressure and shear stress increased simultaneously; the vessel of interest dilated. Similarly, the other arrow

indicates that when an upstream arteriole was occluded, both transmural pressure and shear stress decreased simultaneously; the vessel of interest also dilated.

Figure 4-8 demonstrates the changes in the steady-state resistance of the vessel of interest, M_v plotted as the percentage occlusion of either the parallel arteriole, M_p or the upstream arteriole, M_{in}. In either type of occlusion, the resistance of M_v starts at a higher value and decreases as the parallel or upstream arteriole is progressively occluded from 0% to 100%.

Experimental Results

Real-time changes in response to an in vivo upstream occlusion. Figure 4-9 illustrates the real-time diameter and pseudo shear rate of a representative vessel of interest, B_v, plotted as a function of time after occlusion of the upstream arteriole, B_{in}. When the upstream arteriole, B_{in}, was occluded, the pseudo shear rate in B_v (Fig. 4-9A) decreased almost immediately (<2 seconds) and the arteriole dilated (Fig. 4-9B) in <15 seconds. Although blood flow downstream of the occlusion reduced, collateral flow ensured it never dropped below 20% baseline values in any arteriole studied.

Hemodynamic changes in response to an occlusion: parallel and upstream occlusion. Figure 4-10A represents the percentage change in diameter and pseudo shear rate, when a parallel arteriole was occluded (i.e., B_p in Fig. 4-3B). The parallel occlusion resulted in a significant increase in pseudo shear rate (122$\pm$103%) and significant increase in arteriolar diameter (36$\pm$24%). An increase in diameter was observed in all arterioles in all bats (n=4). Similarly, Fig. 4-10B illustrates the percentage change in arteriolar diameter and pseudo shear rate when an upstream arteriole was occluded (i.e.,

B_{in} in Fig. 4-3C). There was a significant decrease in the pseudo shear rate (70±21%) and a significant concomitant increase in the arteriolar diameter (37±33%). An increase in diameter was observed in all arterioles in all bats (n=8).

DISCUSSION

Theoretical and experimental results reveal that microvessels can functionally "switch" from a predominantly pressure-mediated response to a shear-mediated response to ameliorate compromised perfusion. This functional switch reconciles two competing requirements for arterioles in a microvascular network when challenged with local occlusions. An arteriole has to suppress the shear-mediated response in favor of the pressure-mediated response to dilate appropriately when upstream arterioles are occluded. However, the same arteriole has to suppress the pressure-mediated response in favor of the shear-mediated response to dilate appropriately when parallel arterioles are occluded. A simple mathematical model (Fig. 4-1), based on experimental data and fundamental principles of physics, revealed that the nonlinear pressure-shear-radius relationship (Fig. 4-7) makes this "shear-myogenic switch" possible.

For the vascular "shear-myogenic switch" to ameliorate compromised perfusion, three rules governing network structure must hold. First, there must be appropriate interconnections to permit collateral flow (e.g., B_c in Fig. 4-2). Studies of the microvascular beds of skeletal muscle and skin, for instance have reported the presence of arcades that act as functional collaterals (118). Although it is debated whether or not these vessels chronically adapt to maintain a constant endothelial shear stress (73, 74) or

circumferential wall stress (118), the shear-myogenic switch ensures appropriate adaptation of collaterals in response to acute changes in mechanical stimuli. Second, vessels must normally be appropriately balanced between pressure- and shear-mediated responses, so that they can decrease resistance with either an upstream or parallel occlusion (Fig. 4-8). Third, microvascular occlusions must result in large enough changes in endothelial shear stress or transmural pressure to elicit vasodilation. For instance, the resistance that makes up a collateral pathway (such as through B_c, B_p, and B_v in Fig. 4-2) must have a greater impact on transmural pressure than on shear stress when an upstream arteriole (such as B_{in}) is occluded. Historically, teleological explanations for observed microvascular structure, such as Murray's Energy Law (106, 107), have motivated the search for regulatory mechanisms (74). Although investigators have identified several optimal design principles (106, 107, 121, 123), the shear-myogenic switch is a mechanism that implies a new optimality principle: arterial networks are optimized to withstand acute failure.

Unlike complex mathematical models developed by Pries et al. (31, 119-122), which include four distinct angioadaptive stimuli that effect the radii of hundreds of vessels, our model was strikingly simple (Fig. 4-1). Transmural pressure and shear stress were considered to be the only stimuli; neural and humoral effects were neglected, as well as conducted stimuli. Our model was made even simpler than the coronary microvascular model of Liao et al. (92) by neglecting metabolic factors that could confound our results. Although the topology of our model was based on the branching pattern in a small portion of the Pallid bat wing, its structure is basic enough to

characterize portions of any microvascular network. Similarly, in the attempt to remove all unnecessary complexity in hemodynamics, we assumed constant viscosity and steady, laminar flow. Because the adaptation was based on the Liao et al. model, we assumed their empirical parameters hold for similar-sized arterioles in the bat wing. Although, this model was developed from in vitro data collected from coronary arterioles, it was based on the active and passive pressure curves that are similar to those in other microvascular beds (17). Our intent was not to maximize complexity within the model to accurately simulate network behavior (31, 119-122), but instead to simplify it in order to remove confounders and reveal the mechanism of the "shear-myogenic switch".

In order to observe changes to pressure and shear stress in response to microvascular occlusion without common confounding phenomena, we recently reintroduced the Pallid bat wing model. Transluminating the relatively thin, lightly pigmented wing membrane allows non-invasive measurement of vessel diameter and red blood cell velocity (31). The relatively large surface area-to-mass ratio makes the bat wing structurally analogous to common animal models such as the rat mesentery, hamster cheek pouch, and mouse ear (143, 144). Microvascular regulation in response to interventions, such as increased transmural pressure, de-enervation, local application of heat, increased flow, and topical application of NO-synthase inhibitors, is also similar (143, 144). Most importantly, this animal model was historically used to characterize the myogenic response (31, 34, 35, 69), which yielded behavior qualitatively similar to the assumed vessel model (*Eqs. 4.3-4.5*). In contrast, conventional animal models can pose

challenges to studying the interaction of pressure- and shear-mediated effects. First, intravascular microscopy is usually invasive, and the resulting surgical trauma can cause inflammation, or increase oxygen partial pressure can affect vascular tone (148). Second, invasive studies require anesthesia, which may in itself cause vasodilation (129). Third, many vasculature networks are three-dimensional, which can make mapping the network topology a challenge. Fourth, many tissues have high metabolism rates (56), and therefore are more likely to be affected by metabolites.

Although, metabolic factors are important regulators of blood flow (56), we discounted the effect of metabolic response as the sole cause of the observed arteriolar dilations. First, studies have reported that metabolic factors have a slow response time, taking >30 seconds to yield 50% steady-state dilation (9, 22, 148). The vasodilatory response in our experiments started in less than 2 sec and reached steady-state dilation in <15 sec (Fig. 4-9B). Second, the effect of metabolites is predominant only in very small arterioles downstream of the arterioles we studied (70), and their diffusion from the venules to neighboring arterioles has a relatively small effect on arteriolar diameter (80). Third, the batwing membrane has a very low resting metabolic rate (96), which limits the rate of metabolite production. Fourth, the wing membrane contributes significantly to cutaneous respiration (96). In fact, some species of bats eliminate up to 12% of total CO_2 through their wings at rest (61). Fifth, collateral flow was sufficient to ensure that total flow did not decrease more than 80% in response to an upstream occlusion. Taken together, it is unlikely that a metabolic response is solely responsible for the dilation of the vessels of interest in our study. Similarly, phenomena such as shear-mediated

constriction (10, 48) and the conducted responses (19, 40, 41) are unlikely to explain our observations, since they cannot account for dilation of both downstream and parallel vessels. Such confounding phenomena were intentionally left out of the mathematical model (Fig. 4-1) for the express purpose of proving the shear-myogenic switch alone could be responsible for such dilations.

Studies of the conductance vessels of rabbits seem to indicate that the shear-mediated response overwhelms the pressure-mediated response, resulting in arterial dilation (54, 72, 116). In complete contrast, other studies conducted in isolated coronary vessels (81), cerebral vessels (139) and skeletal vessels (135) seem to indicate that the pressure-mediated response overwhelms shear-mediated responses. Although it is entirely possible that the sensitivities to pressure and shear are very different in different mammals, it has yet to be noted that some experiments are conducted at lower baseline pressures (where the shear-mediated responses are lower) and while others are conducted at higher pressures (where pressure-mediated responses are lower). An alternative interpretation to these reported observations is that they are actually exhibiting a manifestation of the "shear-myogenic switch". If so, then repeating these experiments at different baseline pressures may result in very different results. Johnson and Intagliatta (69) and Kuo et al. (81) speculated that the dominance of a particular response depended on the transmural pressure. Our simple mathematical model revealed a basic mechanism for reconciling these contradictory responses–a nonlinear pressure-shear-radius relationship (Fig. 4-7) that acts as a functional switch.

CHAPTER V

RESEARCH-INTENSIVE COMMUNITIES

INTRODUCTION

Large public research-extensive universities such as Texas A&M University have two primary missions—increase access to education (typically with didactic classes) and perform research (typically in small laboratories) (138). To fulfill these divergent missions, the National Science Foundation (NSF) in particular has been on the forefront of governmental agencies encouraging the integration of research and education. First, all research grants are now required to include "Broader Impacts" that include components such as "advancing discovery and understanding while promoting teaching, training, and learning" or "broadening the participation of underrepresented groups" (25). Second, the NSF invests over $50 million for 4,500 students to attend Research Experience for Undergraduates Sites, primarily to promote careers in research (55). Despite the sustained efforts of federal funding institutions, the Boyer Commission (14) criticized research-extensive universities for not providing "maximal opportunities for intellectual and creative development" by "[learning] through inquiry rather than transmission of knowledge". This Commission suggested making inquiry-based learning the standard, providing a mentor for every student, removing barriers to interdisciplinary education, providing research opportunities for first-year students, enhancing oral and written communication, and educating graduate students as apprentice teachers. However, the Boyer Commission did not provide any means to achieve these self-

described “controversial goals” other than “radical reconstruction” leading to fundamental change in university culture.

Aside from didactic courses covering the theory of research, research training in research-extensive universities is based on an apprenticeship model (23), where students learn by working closely with experienced researchers. Studies of both students and faculty have identified a number of requirements for successful one-on-one research mentoring. First, students collaborate with the faculty to design their own projects. This ensures student participation in all aspects of the project, providing a sense of “ownership” as well as providing exposure higher-level scientific thought (93). Second, students should have opportunities to explore their ingenuity and creativity, and thus have some control over the direction of their activities (115). Third, mentors spend significant time providing not only scientific expertise, but emotional and social support (108). Fourth, students receive technical training and access to state-of-the-art facilities and equipment (59). Taken together, ideal one-on-one mentoring is both time- and resource-intensive.

Successfully sustaining a research program in a research-extensive university has twin requirements: continuity in funding and continuity in expertise (14). A research proposal often needs more than just a novel and important scientific idea, but also preliminary data to successfully secure competitive grant funding (63). Once a grant is successfully obtained, the primary investigator has the difficult task of completing the specific aims within a few years. Given the need to submit continuing proposals as much as a year before the proposed award date, this further compresses the time available to

produce a record of publication and gather preliminary data. This unforgiving timeline requires the labor of technicians, postdoctoral scholars, and graduate students with the specific skills necessary to accomplish the grant's specific aims. On one hand, failure to maintain a pool of skilled labor can endanger continued funding. On the other, failure to secure continued funding can result in loss of skilled labor. A break in either continuity of funding or of expertise thus leads to a vicious cycle and premature termination of a research program. Not only is restarting a research program after a funding hiatus hampered by a lack of resources, senior faculty are often required to increase their university service or teaching load; junior faculty may fail to get tenure (98). With such high stakes, it is not surprising that faculty expressed concerns that working with undergraduates lowers their research productivity, is "risky", requires a "huge time investment" and involves "a lot of hand-holding" (55).

Undergraduate students need to earn a respectable GPA, learn to work and think independently, and choose a career path before graduation. Graduate students, on the other hand, need to publish in the scientific literature, prepare for a career involving collaboration and project management, and complete dissertation research in a reasonable span of time. For promotion and tenure, faculty must recruit skilled labor, maximize research productivity, ensure funding continuity, and perform the minimum required teaching. These conflicting goals manifest as notable failures of the one-on-one research apprenticeship model. First, given the competition for limited research positions, senior undergraduates with high GPAs are often given preference (105). Such selection can have disparate impact on underrepresented minorities (67) and miss a

critical window in the first two years to motivate students to pursue research careers (21, 131) and enhance retention in science majors (104, 108). The few students who do secure positions often assist graduate students by performing low-level scientific tasks or "intellectual bottlewashing" (105). Even vaunted REU Sites change the intention of only 3% of its participants to apply to graduate schools (132), possibly reflecting the tendency to "select the winners" (55). Without a pool of skilled undergraduates to choose from, faculty resort to indirect indices such as GPA and GRE scores (24) to evaluate research potential of graduate school applicants. More importantly, faculty must allocate precious time to train new graduate students. The cost of this delayed development can only be recovered by keeping trained graduate students for as long as possible. Given the need to ensure funding continuity, graduate students are given few opportunities to form collaborations and manage a research program (51). Finally, since faculty perceive they are not rewarded for teaching (14), faculty have few incentives to provide training opportunities for undergraduates, thus leading to a vicious cycle.

In its final analysis, the Boyer Commission did not mince words: "Research universities have often failed, and continue to fail their undergraduate populations; thousands of students graduate without seeing the world-famous professors or tasting genuine research" (14). The challenges to expand undergraduate research opportunities in public research-extensive universities are easily identified. First, there are simply too few faculty to provide one-on-one mentoring to every undergraduate in a large public university. Second, the requirements of one-on-one research mentoring are incompatible with the requirements of sustaining an active research program. As a result, the needs of

the institution, lab directors, graduate students and undergraduates are not being met because they do not share the same goals. Given the difficulty in evaluating educational outcomes for research programs (94, 95), the present work focuses primarily on the development and implementation of a "Research-Intensive Community" model at Texas A&M University. In particular, we will identify how this model successfully integrates research and education by radically increasing the number of undergraduate opportunities and aligning the divergent goals of stakeholders at multiple levels.

METHODS

Model Development

The setting. In the summer of 2003, Dr. Quick (Assistant Professor of Biomedical Engineering, Physiology and Pharmacology), with the support from the Michael E. DeBakey Institute (Directed by Dr. Laine), reintroduced the Pallid bat (*Antrozous pallidus*) as a model for microvascular research. The anatomy of the Pallid bat wing makes it possible to study blood vessels non-invasively via intravital microscopy, thus eliminating the need for terminal experiments (143, 144). Since these animals can be repeatedly studied without harm, they can support a large number of experiments. The original purpose for investing a sizable portion of startup funds in establishing a chronic colony was to test mathematical models of acute and chronic vascular network adaptation (123). Although live animal research has potential for increasing interest in physiology (60), institutional and economic imperatives (2, 130) makes it particularly rare for undergraduate research training.

Inception of a Research-Intensive Community at Texas A&M University. By fall of 2003, despite extensive investment in state-of-the-art microscopy equipment, graduate students skilled in intravital microscopy could not be recruited. Out of a sense of urgency, Dr. Quick (i.e., the lab director) invited 20 undergraduate and graduate students with at least 3.0 GPAs to work in his lab in summer 2004. Due to insufficient management experience, the lab director looked to his own undergraduate training in engineering and created four teams. However, unlike conventional undergraduate engineering teams (44), students invited to the lab were in different stages of training and were studying fields as diverse as biomedical sciences, veterinary medicine, and biomedical engineering. Therefore, each team was made explicitly interdisciplinary and included graduate students. Because it was difficult to create four distinct, well-defined, low-risk projects de novo, each team was charged to develop its own project based on personal interest. Even with the participation of Dr. Stewart (Assistant Research Professor of Physiology and Pharmacology), the ability to provide direct mentoring was limited. Implicitly given freedom to explore, the teams quickly asserted themselves by redefining problems when equipment or lack of expertise became a barrier to progress. Although the teams were not assigned leaders, as the summer progressed the teams became increasingly independent, with more experienced graduate students mentoring undergraduates. Furthermore, because all teams were located in same lab space, they began to spontaneously interact to address common conceptual and experimental challenges. A self organizing, cooperative, multilevel community thus arose with distributed decision making, and Dr. Gatson (Assistant Professor of Sociology) was

invited to observe the developing group and advise the lab director on further development of the emerging model.

Fall 2004. To mimic team structures that arose organically, eight teams were organized, each with one graduate student "team leader" mentoring three undergraduate students. Undergraduates were no longer excluded on the basis of GPA, since it became clear to the lab director that some students with lower GPAs outperformed students with higher GPAs, and students with the highest GPAs did not perform as well as expected. Because teams conducted experiments at different times that accommodated their class schedules, a prototype web-based tool was refined to efficiently facilitate communication between teams, track team activities, and document their actions. Research processes such as reviewing the literature, presenting scientific ideas, and writing conference abstracts, however, required individual attention and a considerable investment of faculty time.

Spring 2005. A majority of students who participated in the fall returned to seed 10 new teams, and the lab director became a "program director". Weekly workshops were incorporated to enrich inter-team interaction, and to allow the program director to disseminate information common to all projects. The practice of weekly "Journal Club" was introduced to ensure that teams became familiar with scientific articles pertaining to their projects. The program director perceived that the performance of veteran first- and second-year undergraduates was better than fourth-year undergraduates who were new to the community. Furthermore, a large number of students graduated at the end of the semester. It thus became clear that there was a benefit to recruiting first- and second-year

students who had the potential to retain corporate knowledge of laboratory practices for multiple semesters.

Fall 2005. With the participation of new graduate students seeking management experience, 12 teams were created. To prepare new leaders to efficiently manage their teams, and to share discovered best-practices amongst veteran leaders, a "Graduate Leadership Forum" was created. Some veteran graduate students, who recognized the potential to expand the scope of their research, requested a second or even third team to manage. Some veteran undergraduate students (with more experience than some new graduate students) also became team leaders.

Spring 2006. With the participation of faculty from other departments who wanted to be part of the rapidly evolving research community, 20 teams were formed. Subsequently, a "Faculty Leadership Forum" was initiated to discuss programmatic issues such as management of research teams and writing grants. The resulting components of the Research-Intensive Community program are illustrated in Fig. 5-1.

Model Analysis

To characterize program efficiency, faculty-to-student ratios were calculated from published reports of representative undergraduate research programs at peer research-extensive universities (138) and compared to the ratios collected over the last three years for the Research-Intensive Community program at Texas A&M University. Furthermore, a survey was taken of the team leaders (n=10) to compare the time spent mentoring a single team to the time spent mentoring multiple teams. To provide evidence of research productivity of our program, the total number of peer-reviewed

abstracts accepted to physiology or bioengineering conferences from fall 2004 to fall 2006 was compiled.

To characterize program growth, the number of undergraduate, graduate, and faculty participants per semester was tabulated. Team leaders were surveyed to determine whether they were willing to recommit to leading teams another semester.

To characterize the goals of the participants within the Research-Intensive Community, semi-structured interviews with team leaders (n=10) and undergraduate students (n=10) were conducted in fall 2007. Consistent with educational psychology (6), individuals express self interest and collective interest as distal goals, which in turn inform the development of proximal sub-goals. The identified sub-goals were thus grouped by individual or collective interests, as well as community education or research practices.

RESULTS

Institutionalized undergraduate research programs at three universities identified as peer institutions (138) (UCLA, University of Wisconsin and University of Michigan) had a faculty-to-student ratio of 1:1.8$\pm$1.3 per semester. In contrast, the Research-Intensive Community program at Texas A&M University had a faculty-to-student ratio that varied between 1:15 to 1:25. Team leaders estimated that mentoring a team of three students required 13$\pm$5 hours/week; mentoring an additional team did not increase this time.

Figure 5-2A demonstrates the growth of undergraduate participation from summer 2004 to spring 2006. Table 1 illustrates the numbers for undergraduate students, graduate students and faculty participating in the Research-Intensive Community each semester. 90% of team leaders expressed a desire to return to the program as a mentor a second semester. Figure 5-2B graphically represents the numbers of students mentored by individual faculty (shown by circles). Faculty new to the community could mentor far fewer than the optimal number of students by leveraging the infrastructure of the established Research-Intensive Community.

Interviews of the undergraduate students indicated that their goals (Table 5-2) were primarily characterized by individual self-interests. The Research-Intensive Community program helped them gain an authentic research experience, enhance academic credentials, make career-related decisions, establish relationships with research professionals, and increase familiarity with particular subjects while developing a capacity for critical problem-solving.

Interviews of the graduate students (Table 5-3) revealed that participation in the Research-Intensive Community program played a significant role in publishing conference abstracts and manuscripts, developing leadership skills to manage diverse teams, and conducting novel research to broaden experience and improve their curriculum vitae. Unlike undergraduates, graduate students also expressed collective interests as a result of their participation in the Research-Intensive Community program. Identified collective interests included mentoring undergraduates to acquire research skills, helping the program director with acquiring tenure and funding, exploring

unanswered questions in science, as well as conducting research to improve the lives of others.

Through his participation in the Research-Intensive Community program, the program director provided graduate students with research and management training. Furthermore, he was able to identify and recruit new graduate students from a pool of particularly skilled undergraduates based on a known history of research performance. The Research-Intensive Community model generated 113 conference-related publications from fall 2004 to fall 2006 with undergraduate students as first authors or co-authors.

DISCUSSION

In their ethnographic study of communities of practice, Lave and Wenger (90) characterize learning curricula as those that allow individuals to "improvise" ways of relating the core knowledge of a community to their own goals for participation. Two social conditions are required for inquiry activities to be characterized as authentic learning activities. First, all members occupy empowered positions. In the Research-Intensive Community at Texas A&M University, veterans and neophytes negotiate the roles, norms, and meanings of doing research. Participants select projects, determine the manner of their participation, and even disinvest from projects that no longer satisfy their goals. Second, members achieve self-efficacy through the communicative practices of the community. In the Research-Intensive Community program, online tools, weekly workshops, journal clubs, and forums emerged as sites for improvisation, where the

competency of each members' performance could be judged by others. Beyond demonstrating research productivity, the Research-Intensive Community model captures the essential characteristics for authentic activities within a learning community.

The Research-Intensive Community model exhibits a number of characteristics that make it a complex adaptive system; it consists of diverse interconnected agents that interact and respond to their local environments (1, 91), not unlike vascular networks studied by the program director (123). The fundamental organizational unit of the research-intensive community is the team, consisting of a broadly diverse group of three undergraduates led by a team leader. As with any complex adaptive system, control is highly decentralized (91). Charged with formulating projects, designing novel experimental techniques, and solving problems that arise in the course of the project, teams exercised a high degree of autonomy. Like other complex adaptive systems that tend to evolve, the Research-Intensive Community program at Texas A&M University exhibited emergent properties arising from the cooperation and interaction of participants. Teams began coordinating their activities through specialized online tools, weekly workshops, journal clubs and other team meetings, and forums. In fact, it is the fundamental nature of the model as a complex adaptive system that allowed it to evolve since its inception in the summer of 2004, changing and learning from experience gained from competing best practices that were developed by each team. In general, complex adaptive systems tend to be resilient, fill new niches, and reproduce (39). The Research-Intensive Community model as implemented at Texas A&M University has exhibited each of these qualities, giving us good reason to believe that the program is transferable

to other universities. Of course, all complex adaptive systems require an input of energy for emergent properties to manifest (20). In the case of the Research-Intensive Community, many of the new programmatic elements and management tools were designed specifically to reduce the administrative input of the lab director and team leaders. The additional time required to administer the Research-Intensive Community program was offset by course credit for graduate students and teaching credit for the lab director.

The development of the large-scale Research Intensive Community program at Texas A&M University required new tools designed specifically to 1) maximize efficiency of program management, 2) enhance communication and community formation, and 3) synergize research and educational activities. Our particular solution was to develop an online portal called "eBat". This portal allows participants to post comments online, and has advantages beyond email and traditional electronic bulletin boards (111). Members can create and maintain a central online presence with archived spontaneous and deliberative communications. This freedom allows participants to 1) develop a sense of ownership of a communal space, 2) participate in one or more interlocking discussions, and 3) contribute, even if they are not physically present in the lab. Space is dedicated for informal daily reports of experimental findings, difficulties and questions; formal weekly updates; and any "discoveries," whether or not verified as a novel finding by detailed literature review. Ideas that are recognized as novel and scientifically important enough to warrant development of peer-reviewed publication are transferred to the "Manuscript Builder". This particular tool allows uploading of

abstracts, outlines, rough drafts, final drafts, and page proofs of manuscripts in development. Not only can new community members learn how published manuscripts evolve, they are provided guidance for constructively criticizing manuscripts in preparation. With integrated forms for applying to the program, reporting problems, and evaluating performance of undergraduate students, the online portal reduces time spent on administrative activities. Taken together, these tools are manifestations of governing principles of openness (e.g., making "thinking visible" (23, 49, 110) for neophytes and education researchers), authenticity (e.g., avoiding educational activities that do not enhance research productivity) and synergy (i.e., ensuring activities serve both research and education).

The Council of Undergraduate Research (CUR) is an example of a non-profit organization that complements the NSF's attempts to establish, formalize and expand undergraduate research opportunities. According to CUR (57), institutionalizing a research program involves creating 1) a sustainable undergraduate research program based on best practices 2) a community of faculty and administrators that share a mutual interest in undergraduate research, and 3) a culture that supports undergraduate research. Several well-funded universities such as Caltech and MIT have successfully institutionalized undergraduate research programs (105), primarily by leveraging existing research opportunities. The low faculty-to-student ratios at most large public universities (105), however, can limit opportunities for one-on-one research mentoring. The Research-Intensive Community program at Texas A&M University, however, provides a novel means to radically increase the number of undergraduates that can be

supported by a single faculty member, and is inherently scalable (Fig 5-2B). In addition, it has three critical aspects which do not require formal institutionalization. First, because it is distributed, yet has internal mechanisms to share ideas recognized to have value, a sustainable organization based on best practices emerges. Second, because education activities have the potential to produce fundable research, it can form a community of faculty and administrators that share a mutual interest in undergraduate research. Third, because the model aligns the goals of undergraduates with graduate students and faculty, it yields an environment that supports undergraduate research—without requiring a radical change in university culture (14). The Research-Intensive Community model thus may provide the means to fulfill the promise of public research-extensive universities as first conceived by the Morrill Act—providing educational opportunities for all (67).

CHAPTER VI

CONCLUSIONS

Generating acute edema in both control and chronic animals resulted in increased stiffness of the left ventricular chamber. Chronically edematous hearts had higher left ventricular chamber compliance when compared to non-edematous control hearts. Compared to control animals, the percentage of type III collagen in the left ventricles of chronically edematous hearts was significantly higher, and type I collagen was significantly lower.

Theoretical and experimental results reveal that microvessels can functionally "switch" from a predominantly pressure-mediated response to a shear-mediated response to ameliorate compromised perfusion. This functional switch reconciles two competing requirements for arterioles in a microvascular network when challenged with local occlusions. An arteriole has to suppress the shear-mediated response in favor of the pressure-mediated response to dilate appropriately when upstream arterioles are occluded. However, the same arteriole has to suppress the pressure-mediated response in favor of the shear-mediated response to dilate appropriately when parallel arterioles are occluded. A simple mathematical model based on experimental data and fundamental principles of physics, revealed that the nonlinear pressure-shear-radius relationship makes this "shear-myogenic switch" possible.

The fundamental unit of the RIC model is a team consisting of a graduate student and three undergraduates from different fields. Undergraduate workshops, graduate and

faculty leadership forums and computer-mediated communication provide novel tools to optimize programmatic efficiency, enhance cooperation within and amongst teams, and sustain a multilevel, interdisciplinary community of scholars dedicated to collective research-related interests. While the model radically increases the number of undergraduate students supported by a single faculty member, the inherent resilience and scalability of this complex adaptive system enables it to expand without formal institutionalization.

Taken together, the heart, microvasculature as well as Research-Intensive Communities can be characterized as complex adaptive systems.

REFERENCES

1. **Allen PM.** A complex systems approach to learning in adaptive networks. *International Journal of Innovation Management* 5: 149-180, 2001.
2. **Ammons SW.** Use of live animals in the curricula of U.S. medical schools in 1994. *Acad Med* 70: 740-743, 1995.
3. **Atance J, Yost MJ, Carver W.** Influence of the extracellular matrix on the regulation of cardiac fibroblast behavior by mechanical stretch. *J Cell Physiol* 200: 377-386, 2004.
4. **Babikian VL, Caplan LR.** Brain embolism is a dynamic process with variable characteristics. *Neurology* 54: 797-801, 2000.
5. **Badenhorst D, Maseko M, Tsotetsi OJ, Naidoo A, Brooksbank R, Norton GR, Woodiwiss AJ.** Cross-linking influences the impact of quantitative changes in myocardial collagen on cardiac stiffness and remodeling in hypertension in rats. *Cardiovasc Res* 57: 632-641, 2003.
6. **Bandura A.** *Self-efficacy: the Exercise of Control*. New York: W.H. Freeman. 1997.
7. **Bashey RI, Bashey HM, Jimenez SA.** Characterization of pepsin-solubilized bovine heart-valve collagen. *Biochem J* 173: 885-894, 1978.
8. **Bayliss WM.** On the local reactions of the arterial wall to changes of internal pressure. *J Physiol* 28: 220-231, 1902.
9. **Berry KL, Skyrme-Jones RA, Meredith IT.** Occlusion cuff position is an important determinant of the time course and magnitude of human brachial artery flow-mediated dilation. *Clin Sci (Lond)* 99: 261-267, 2000.
10. **Bevan JA.** Shear stress, the endothelium and the balance between flow-induced contraction and dilation in animals and man. *Int J Microcirc Clin Exp* 17: 248-256, 1997.
11. **Bishop JJ, Popel AS, Intaglietta M, Johnson PC.** Rheological effects of red blood cell aggregation in the venous network: a review of recent studies. *Biorheology* 38: 263-274, 2001.
12. **Bishop SP, Cole CR.** Production of externally controlled progressive pulmonic stenosis in the dog. *J Appl Physiol* 26: 659-663, 1969.
13. **Borgstrom P, Grande PO, Mellander S.** A mathematical description of the myogenic response in the microcirculation. *Acta Physiol Scand* 116: 363-376, 1982.
14. **Boyer Commission on Educating Undergraduates in the Research University.** Reinventing undergraduate education: a blueprint for America's research universities, Stoney Brook, NY, 1998.
15. **Brower GL, Gardner JD, Forman MF, Murray DB, Voloshenyuk T, Levick SP, Janicki JS.** The relationship between myocardial extracellular matrix remodeling and ventricular function. *Eur J Cardiothorac Surg* 30: 604-610, 2006.

16. **Burgess ML, Buggy J, Price RL, Abel FL, Terracio L, Samarel AM, Borg TK.** Exercise- and hypertension-induced collagen changes are related to left ventricular function in rat hearts. *Am J Physiol Heart Circ Physiol* 270: H151-159, 1996.
17. **Carlson BE, Secomb TW.** A theoretical model for the myogenic response based on the length-tension characteristics of vascular smooth muscle. *Microcirculation* 12: 327-338, 2005.
18. **Carver W, Nagpal ML, Nachtigal M, Borg TK, Terracio L.** Collagen expression in mechanically stimulated cardiac fibroblasts. *Circ Res* 69: 116-122, 1991.
19. **Chen Y, Rivers RJ.** Arteriolar occlusion causes independent cellular responses in endothelium and smooth muscle. *Microcirculation* 9: 353-362, 2002.
20. **Choi TY, Dooley KJ, Rungtusanatham M.** Supply networks and complex adaptive systems: control versus emergence. *Journal of Operations Management* 19: 351-366, 2001.
21. **Cisnerosa RM, Salisbury-Glennonb JD, Anderson-Harper HM.** Status of problem-based learning research in pharmacy education: a call for future research. *Am J Pharm Educ* 66: 19-26, 2002.
22. **Clifford PS, Hellsten Y.** Vasodilatory mechanisms in contracting skeletal muscle. *J Appl Physiol* 97: 393-403, 2004.
23. **Collins A, Brown JS, Holum A.** Cognitive apprenticeship: making thinking visible. *American Educator*, Winter: 6-46, 1991.
24. **Cooksey L, Stenning WF.** The empirical impact of the graduate record examination and grade point average on entry and success in graduate school at Texas A&M University. Texas A&M University, 1981.
25. **Cordes D, Evans DL, Frair K, Froyd J.** The NSF Foundation Coalition: the first five years. *Journal of Engineering Education,* 88: 73-77, 1999.
26. **Cornelissen AJ, Dankelman J, VanBavel E, Spaan JA.** Balance between myogenic, flow-dependent, and metabolic flow control in coronary arterial tree: a model study. *Am J Physiol Heart Circ Physiol* 282: H2224-2237, 2002.
27. **Cornelissen AJ, Dankelman J, VanBavel E, Stassen HG, Spaan JA.** Myogenic reactivity and resistance distribution in the coronary arterial tree: a model study. *Am J Physiol Heart Circ Physiol* 278: H1490-1499, 2000.
28. **Davis JO, Hyat RE, Howell DS.** Right-sided congestive heart failure in dogs produced by controlled progressive constriction of the pulmonary artery. *Circ Res* 3: 252-258, 1955.
29. **Davis KL, Laine GA, Geissler HJ, Mehlhorn U, Brennan M, Allen SJ.** Effects of myocardial edema on the development of myocardial interstitial fibrosis. *Microcirculation* 7: 269-280, 2000.
30. **Davis KL, Mehlhorn U, Laine GA, Allen SJ.** Myocardial edema, left ventricular function, and pulmonary hypertension. *J Appl Physiol* 78: 132-137, 1995.

31. **Davis MJ.** Microvascular control of capillary pressure during increases in local arterial and venous pressure. *Am J Physiol Heart Circ Physiol* 254: H772-784, 1988.
32. **Davis MJ, Hill MA.** Signaling mechanisms underlying the vascular myogenic response. *Physiol Rev* 79: 387-423, 1999.
33. **Davis MJ, Shi X, Sikes PJ.** Modulation of bat wing venule contraction by transmural pressure changes. *Am J Physiol Heart Circ Physiol* 262: H625-634, 1992.
34. **Davis MJ, Sikes PJ.** Myogenic responses of isolated arterioles: test for a rate-sensitive mechanism. *Am J Physiol Heart Circ Physiol* 259: H1890-1900, 1990.
35. **Davis MJ, Sikes PJ.** A rate-sensitive component to the myogenic response is absent from bat wing arterioles. *Am J Physiol Heart Circ Physiol* 256: H32-40, 1989.
36. **de Wit C, Jahrbeck B, Schafer C, Bolz SS, Pohl U.** Nitric oxide opposes myogenic pressure responses predominantly in large arterioles in vivo. *Hypertension* 31: 787-794, 1998.
37. **Detwiler PW, Nicolosi AC, Weng ZC, Spotnitz HM.** Effects of perfusion-induced edema on diastolic stress-strain relations in intact swine papillary muscle. *J Thorac Cardiovasc Surg* 108: 467-476, 1994.
38. **Doering CW, Jalil JE, Janicki JS, Pick R, Aghili S, Abrahams C, Weber KT.** Collagen network remodelling and diastolic stiffness of the rat left ventricle with pressure overload hypertrophy. *Cardiovasc Res* 22: 686-695, 1988.
39. **Dooley KJ.** A complex adaptive systems model of organization change. *Nonlinear Dynamics, Psychol Life Sci* 1: 69-97, 1997.
40. **Dora KA, Damon DN, Duling BR.** Microvascular dilation in response to occlusion: a coordinating role for conducted vasomotor responses. *Am J Physiol Heart Circ Physiol* 279: H279-284, 2000.
41. **Doyle MP, Duling BR.** Acetylcholine induces conducted vasodilation by nitric oxide-dependent and -independent mechanisms. *Am J Physiol Heart Circ Physiol* 272: H1364-1371, 1997.
42. **Drzewiecki G, Field S, Moubarak I, Li JK.** Vessel growth and collapsible pressure-area relationship. *Am J Physiol Heart Circ Physiol* 273: H2030-2043, 1997.
43. **Drzewiecki G, Pilla JJ.** Noninvasive measurement of the human brachial artery pressure-area relation in collapse and hypertension. *Ann Biomed Eng* 26: 965-974, 1998.
44. **Feisel LD, Rosa AJ.** The role of the laboratory in undergraduate engineering education. *Journal of Engineering Education* 94: 121-130, 2005.
45. **Fischer UM, Cox CS, Jr., Stewart RH, Laine GA, Allen SJ.** Impact of acute myocardial edema on left ventricular function. *J Invest Surg* 19: 31-38, 2006.
46. **Fridez P, Zulliger M, Bobard F, Montorzi G, Miyazaki H, Hayashi K, Stergiopulos N.** Geometrical, functional, and histomorphometric adaptation of rat carotid artery in induced hypertension. *J Biomech* 36: 671-680, 2003.

47. **Frisbee JC.** Regulation of in situ skeletal muscle arteriolar tone: interactions between two parameters. *Microcirculation* 9: 443-462, 2002.
48. **Garcia-Roldan JL, Bevan JA.** Augmentation of endothelium-independent flow constriction in pial arteries at high intravascular pressures. *Hypertension* 17: 870-874, 1991.
49. **Gatson SN, Stewart RH, Laine GA, Quick CM.** Optimizing efficiency of undergraduate research experiences with research-intensive communities. *Biomedical Engineering Society*: Chicago, IL, (Abstract #907) 2006.
50. **Geissler HJ, Davis KL, Buja LM, Laine GA, Brennan ML, Mehlhorn U, Allen SJ.** Esmolol and cardiopulmonary bypass during reperfusion reduce myocardial infarct size in dogs. *Ann Thorac Surg* 72: 1964-1969, 2001.
51. **Gonzalez C.** Undergraduate research, graduate mentoring, and the university's mission. *Science* 293: 1624-1626, 2001.
52. **Gore RW, Bohlen HG.** Pressure regulation in the microcirculation. *Fed Proc* 34: 2031-2037, 1975.
53. **Green DJ, O'Driscoll G, Blanksby BA, Taylor RR.** Control of skeletal muscle blood flow during dynamic exercise: contribution of endothelium-derived nitric oxide. *Sports Med* 21: 119-146, 1996.
54. **Griffith TM, Edwards DH.** Myogenic autoregulation of flow may be inversely related to endothelium-derived relaxing factor activity. *Am J Physiol Heart Circ Physiol* 258: H1171-1180, 1990.
55. **Guterman L.** What good is undergraduate research, anyway? *Chron High Educ* 53: A12, 2007.
56. **Haddy FJ, Scott JB.** Metabolically linked vasoactive chemicals in local regulation of blood flow. *Physiol Rev* 48: 688-707, 1968.
57. **Hakim TM.** At the interface of scholarship and teaching: how to develop and administer institutional undergraduate research programs. *Council of Undergraduate Research*, July 2000.
58. **Harrigan TP.** Regulatory interaction between myogenic and shear-sensitive arterial segments: conditions for stable steady states. *Ann Biomed Eng* 25: 635-643, 1997.
59. **Hathaway RS, Nagda BA, Gregerman SR.** The relationship of undergraduate research participation to graduate and professional education pursuit: an empirical study. *Journal of College Student Development* 43: 614-631, 2002.
60. **Hedlund CS, Hosgood G, Naugler S.** Surgical education: attitudes toward animal use in teaching surgery at Louisiana State University. *J Vet Med Educ* 29: 50-55, 2002.
61. **Herreid CF, 2nd, Bretz WL, Schmidt-Nielsen K.** Cutaneous gas exchange in bats. *Am J Physiol* 215: 506-508, 1968.
62. **Hill AJ, Ahlberg SE, Wilkoff BL, Iaizzo PA.** Dynamic obstruction to coronary sinus access: the Thebesian valve. *Heart Rhythm* 3: 1240-1241, 2006.
63. **Inouye SK, Fiellin DA.** An evidence-based guide to writing grant proposals for clinical research. *Ann Intern Med* 142: 274-282, 2005.

64. **Jain AK, Smith EJ, Rothman MT.** the coronary venous system: an alternative route of access to the myocardium. *J Invasive Cardiol* 18: 563-568, 2006.
65. **Janicki JS.** Myocardial collagen remodeling and left ventricular diastolic function. *Braz J Med Biol Res* 25: 975-982, 1992.
66. **Janicki JS, Brower GL.** The role of myocardial fibrillar collagen in ventricular remodeling and function. *J Card Fail* 8: S319-325, 2002.
67. **Jewell JO.** An unfinished mission: affirmative action, minority admissions, and the politics of mission at the University of California, 1868-1997. *Journal of Negro Education* 69: 38-48, 2000.
68. **Jimenez SA, Bashey RI.** Solubilization of bovine heart-value collagen. *Biochem J* 173: 337-340, 1978.
69. **Johnson PC, Intaglietta M.** Contributions of pressure and flow sensitivity to autoregulation in mesenteric arterioles. *Am J Physiol* 231: 1686-1698, 1976.
70. **Jones CJ, Kuo L, Davis MJ, Chilian WM.** Distribution and control of coronary microvascular resistance. *Adv Exp Med Biol* 346: 181-188, 1993.
71. **Jones CJ, Kuo L, Davis MJ, Chilian WM.** Myogenic and flow-dependent control mechanisms in the coronary microcirculation. *Basic Res Cardiol* 88: 2-10, 1993.
72. **Juncos LA, Garvin J, Carretero OA, Ito S.** Flow modulates myogenic responses in isolated microperfused rabbit afferent arterioles via endothelium-derived nitric oxide. *J Clin Invest* 95: 2741-2748, 1995.
73. **Kamiya A, Bukhari R, Togawa T.** Adaptive regulation of wall shear stress optimizing vascular tree function. *Bull Math Biol* 46: 127-137, 1984.
74. **Kassab GS, Fung YC.** The pattern of coronary arteriolar bifurcations and the uniform shear hypothesis. *Ann Biomed Eng* 23: 13-20, 1995.
75. **Koller A, Kaley G.** Endothelial regulation of wall shear stress and blood flow in skeletal muscle microcirculation. *Am J Physiol Heart Circ Physiol* 260: H862-868, 1991.
76. **Koller A, Messina EJ, Wolin MS, Kaley G.** Effects of endothelial impairment on arteriolar dilator responses in vivo. *Am J Physiol Heart Circ Physiol* 257: H1485-1489, 1989.
77. **Koller A, Sun D, Kaley G.** Role of shear stress and endothelial prostaglandins in flow- and viscosity-induced dilation of arterioles in vitro. *Circ Res* 72: 1276-1284, 1993.
78. **Kong D, Kong X, Wang L.** Effect of cardiac lymph flow obstruction on cardiac collagen synthesis and interstitial fibrosis. *Physiol Res* 55: 253-258, 2006.
79. **Kong XQ, Wang LX, Kong DG.** Cardiac lymphatic interruption is a major cause for allograft failure after cardiac transplantation. *Lymphat Res Biol* 5: 45-47, 2007.
80. **Kopyltsov AV, Groebe K.** Mathematical modeling of local regulation of blood flow by veno-arterial diffusion of vasoactive metabolites. *Adv Exp Med Biol* 411: 303-311, 1997.

81. **Kuo L, Chilian WM, Davis MJ.** Interaction of pressure- and flow-induced responses in porcine coronary resistance vessels. *Am J Physiol Heart Circ Physiol* 261: H1706-1715, 1991.
82. **Kuo L, Davis MJ, Chilian WM.** Longitudinal gradients for endothelium-dependent and -independent vascular responses in the coronary microcirculation. *Circulation* 92: 518-525, 1995.
83. **Laine GA.** Microvascular changes in the heart during chronic arterial hypertension. *Circ Res* 62: 953-960, 1988.
84. **Laine GA.** Change in (dP/dt)max as an index of myocardial microvascular permeability. *Circ Res* 61: 203-208, 1987.
85. **Laine GA, Allen SJ.** Left ventricular myocardial edema. Lymph flow, interstitial fibrosis, and cardiac function. *Circ Res* 68: 1713-1721, 1991.
86. **Laine GA, Allen SJ, Katz J, Gabel JC, Drake RE.** Effect of systemic venous pressure elevation on lymph flow and lung edema formation. *J Appl Physiol* 61: 1634-1638, 1986.
87. **Laine GA, Granger HJ.** Microvascular, interstitial, and lymphatic interactions in normal heart. *Am J Physiol Heart Circ Physiol* 249: H834-842, 1985.
88. **Laine GA, Hall JT, Laine SH, Granger J.** Transsinusoidal fluid dynamics in canine liver during venous hypertension. *Circ Res* 45: 317-323, 1979.
89. **Laurent GJ.** Dynamic state of collagen: pathways of collagen degradation in vivo and their possible role in regulation of collagen mass. *Am J Physiol Heart Circ Physiol* 252: C1-9, 1987.
90. **Lave J, Wenger E.** *Situated Learning: Legitimate Peripheral Participation.* Cambridge: Cambridge University Press, 1991.
91. **Levin SA.** Complex adaptive systems: exploring the known, the unknown and the unknowable. *Bulletin of the American Mathematical Society* 40: 3-19, 2002.
92. **Liao JC, Kuo L.** Interaction between adenosine and flow-induced dilation in coronary microvascular network. *Am J Physiol Heart Circ Physiol* 272: H1571-1581, 1997.
93. **Lopatto D.** The essential features of undergraduate research. *Council on Undergraduate Research Quaterly* March: 139-142, 2003.
94. **Lopatto D.** Survey of undergraduate research experiences (SURE): first findings. *Cell Biol Educ* 3: 270-277, 2004.
95. **Lopatto D.** Undergraduate research experiences support science career decisions and active learning. *CBE Life Sci Educ* 6: 297-306, 2007.
96. **Makanya AN, Mortola JP.** The structural design of the bat wing web and its possible role in gas exchange. *J Anat* 211: 687-697, 2007.
97. **McAnulty RJ, Laurent GJ.** Collagen synthesis and degradation in vivo. Evidence for rapid rates of collagen turnover with extensive degradation of newly synthesized collagen in tissues of the adult rat. *Coll Relat Res* 7: 93-104, 1987.
98. **McCabe LL, McCabe ER.** *How to Succeed in Academics*. Academic Press: San Diego, 2000.

99. **McGahren ED, Dora KA, Damon DN, Duling BR.** A test of the role of flow-dependent dilation in arteriolar responses to occlusion. *Am J Physiol Heart Circ Physiol* 272: H714-721, 1997.
100. **Mehlhorn U, Davis KL, Burke EJ, Adams D, Laine GA, Allen SJ.** Impact of cardiopulmonary bypass and cardioplegic arrest on myocardial lymphatic function. *Am J Physiol Heart Circ Physiol* 268: H178-183, 1995.
101. **Mehlhorn U, Davis KL, Laine GA, Geissler HJ, Allen SJ.** Myocardial fluid balance in acute hypertension. *Microcirculation* 3: 371-378, 1996.
102. **Meininger GA, Mack CA, Fehr KL, Bohlen HG.** Myogenic vasoregulation overrides local metabolic control in resting rat skeletal muscle. *Circ Res* 60: 861-870, 1987.
103. **Meisner J, Weaver AL, Quick CM.** Real-time in vivo microvascular diameter tracking system. *22nd Annual Houston Conference in Biomedical Research,* Houston, TX. *Houston Society for Engineering in Medicine and Biology*: 64, 2005.
104. **Melton G, Pederson-Gallegos L, Donohue R, Hunter AB.** SOARS: a research-with-evaluation study of a multi-year research and mentoring program for underrepresented students in science. Center to Advance Research and Teaching in the Social Sciences, University of Colorado, Boulder, 2005.
105. **Merkel CA.** Undergraduate research at six research universities: a pilot study for the Association of American Universities. Association of American Universities, 2001.
106. **Murray CD.** The physiological principle of minimum work: I. the vascular system and the cost of blood volume. *Proc Natl Acad Sci USA* 12: 207-214, 1926.
107. **Murray CD.** The physiological principle of minimum work: II. oxygen exchange in capillaries. *Proc Natl Acad Sci USA* 12: 299-304, 1926.
108. **Nagda BA, Gregerman SR, Jonides J, von Hippel W, Lerner JS.** Undergraduate student-faculty research partnerships affect student retention. *Review of Higher Education* 22: 55-72, 1998.
109. **Neter J, Wasserman W.** *Applied Linear Statistical Models*. Homewood, IL: Irwin, 1974.
110. **Nordt M, Gatson SN, Furuta R, Quick CM.** Integrating research and teaching in ebat. *Third Annual TAMUS Pathways Research Symposium,* Kingsville, TX. *TAMUS* 3: 15-16, 2005.
111. **Nordt M, Meisner J, Dongaonkar R, Quick CM, Gatson SN, Karadkar U, Furuta R.** eBat: a technology-enriched life sciences research community. *ASIST*, 43: 1-17, 2006.
112. **Norton GR, Tsotetsi J, Trifunovic B, Hartford C, Candy GP, Woodiwiss AJ.** Myocardial stiffness is attributed to alterations in cross-linked collagen rather than total collagen or phenotypes in spontaneously hypertensive rats. *Circulation* 96: 1991-1998, 1997.

113. **Oien AH, Aukland K.** A mathematical analysis of the myogenic hypothesis with special reference to autoregulation of renal blood flow. *Circ Res* 52: 241-252, 1983.
114. **Olivetti G, Ricci R, Lagrasta C, Maniga E, Sonnenblick EH, Anversa P.** Cellular basis of wall remodeling in long-term pressure overload-induced right ventricular hypertrophy in rats. *Circ Res* 63: 648-657, 1988.
115. **Peppas NA.** Student preparation for graduate school through undergraduate research. *Chemical Engineering Education* 15: 135-137, 1981.
116. **Pohl U, Herlan K, Huang A, Bassenge E.** EDRF-mediated shear-induced dilation opposes myogenic vasoconstriction in small rabbit arteries. *Am J Physiol Heart Circ Physiol* 261: H2016-2023, 1991.
117. **Pratt JW, Schertel ER, Schaefer SL, Esham KE, McClure DE, Heck CF, Myerowitz PD.** Acute transient coronary sinus hypertension impairs left ventricular function and induces myocardial edema. *Am J Physiol Heart Circ Physiol* 271: H834-841, 1996.
118. **Price RJ, Less JR, Van Gieson EJ, Skalak TC.** Hemodynamic stresses and structural remodeling of anastomosing arteriolar networks: design principles of collateral arterioles. *Microcirculation* 9: 111-124, 2002.
119. **Pries AR, Secomb TW.** Microcirculatory network structures and models. *Ann Biomed Eng* 28: 916-921, 2000.
120. **Pries AR, Secomb TW, Gaehtgens P.** Structural adaptation and stability of microvascular networks: theory and simulations. *Am J Physiol Heart Circ Physiol* 275: H349-360, 1998.
121. **Pries AR, Secomb TW, Gaehtgens P.** Design principles of vascular beds. *Circ Res* 77: 1017-1023, 1995.
122. **Pries AR, Secomb TW, Gaehtgens P, Gross JF.** Blood flow in microvascular networks. Experiments and simulation. *Circ Res* 67: 826-834, 1990.
123. **Quick CM, Young WL, Leonard EF, Joshi S, Gao E, Hashimoto T.** Model of structural and functional adaptation of small conductance vessels to arterial hypotension. *Am J Physiol Heart Circ Physiol* 279: H1645-1653, 2000.
124. **Radhakrishnan RS, Radhakrishnan HR, Xue H, Moore-Olufemi SD, Mathur AB, Weisbrodt NW, Moore FA, Allen SJ, Laine GA, Cox CS, Jr.** Hypertonic saline reverses stiffness in a Sprague-Dawley rat model of acute intestinal edema, leading to improved intestinal function. *Crit Care Med* 35: 538-543, 2007.
125. **Radhakrishnan RS, Xue H, Moore-Olufemi SD, Weisbrodt NW, Moore FA, Allen SJ, Laine GA, Cox CS, Jr.** Hypertonic saline resuscitation prevents hydrostatically induced intestinal edema and ileus. *Crit Care Med* 34: 1713-1718, 2006.
126. **Radhakrishnan RS, Xue H, Weisbrodt N, Moore FA, Allen SJ, Laine GA, Cox CS, Jr.** Resuscitation-induced intestinal edema decreases the stiffness and residual stress of the intestine. *Shock* 24: 165-170, 2005.
127. **Schaper W, Ito WD.** Molecular mechanisms of coronary collateral vessel growth. *Circ Res* 79: 911-919, 1996.

128. **Schubert R, Mulvany MJ.** The myogenic response: established facts and attractive hypotheses. *Clin Sci (Lond)* 96: 313-326, 1999.
129. **Schwinn DA, McIntyre RW, Reves JG.** Isoflurane-induced vasodilation: role of the alpha-adrenergic nervous system. *Anesth Analg* 71: 451-459, 1990.
130. **Sechzer JA.** Historical issues concerning animal experimentation in the United States. *Soc Sci Med* 15: 13-17, 1981.
131. **Sedlacek WE.** Admissions in higher education: measuring cognitive and noncognitive variables. *Minorities in Higher Education 1997-98 Sixteenth Annual Status Report*: 47-71, 1998.
132. **Seymour EL, Hunter AB, Laursen S, DeAntoni T.** Establishing the benefits of research experiences for undergraduates: first findings from a three-year study. *Sci Educ* 88: 493-594, 2004.
133. **Smiesko V, Lang DJ, Johnson PC.** Dilator response of rat mesenteric arcading arterioles to increased blood flow velocity. *Am J Physiol Heart Circ Physiol* 257: H1958-1965, 1989.
134. **Spotnitz HM, Hsu DT.** Myocardial edema: importance in the study of left ventricular function. *Adv Card Surg* 5: 1-25, 1994.
135. **Sun D, Huang A, Koller A, Kaley G.** Flow-dependent dilation and myogenic constriction interact to establish the resistance of skeletal muscle arterioles. *Microcirculation* 2: 289-295, 1995.
136. **Swank RL, Seaman GV.** Microfiltration and microemboli: a history. *Transfusion* 40: 114-119, 2000.
137. **Sykes B, Puddle B, Francis M, Smith R.** The estimation of two collagens from human dermis by interrupted gel electrophoresis. *Biochem Biophys Res Commun* 72: 1472-1480, 1976.
138. **Texas A&M University.** Vision 2020: creating a culture of excellence for the 21st century. Texas A&M University, College Station, TX, 2002.
139. **Thorin-Trescases N, Bevan JA.** High levels of myogenic tone antagonize the dilator response to flow of small rabbit cerebral arteries. *Stroke* 29: 1194-1201, 1998.
140. **Ursino M, Lodi CA.** A simple mathematical model of the interaction between intracranial pressure and cerebral hemodynamics. *J Appl Physiol* 82: 1256-1269, 1997.
141. **Weber KT, Jalil JE, Janicki JS, Pick R.** Myocardial collagen remodeling in pressure overload hypertrophy. A case for interstitial heart disease. *Am J Hypertens* 2: 931-940, 1989.
142. **Weber KT, Janicki JS, Shroff SG, Pick R, Chen RM, Bashey RI.** Collagen remodeling of the pressure-overloaded, hypertrophied nonhuman primate myocardium. *Circ Res* 62: 757-765, 1988.
143. **Widmer RJ, Laurinec JE, Young MF, Laine GA, Quick CM.** Local heat produces a shear-mediated biphasic response in the thermoregulatory microcirculation of the Pallid bat wing. *Am J Physiol Regul Integr Comp Physiol* 291: R625-632, 2006.

144. **Widmer RJ, Stewart RH, Young MF, Laurinec JE, Laine GA, Quick CM.** Application of local heat induces capillary recruitment in the Pallid bat wing. *Am J Physiol Regul Integr Comp Physiol* 292: R2312-2317, 2007.
145. **Wunsch SA, Muller-Delp J, Delp MD.** Time course of vasodilatory responses in skeletal muscle arterioles: role in hyperemia at onset of exercise. *Am J Physiol Heart Circ Physiol* 279: H1715-1723, 2000.
146. **Yamamoto K, Masuyama T, Sakata Y, Nishikawa N, Mano T, Yoshida J, Miwa T, Sugawara M, Yamaguchi Y, Ookawara T, Suzuki K, Hori M.** Myocardial stiffness is determined by ventricular fibrosis, but not by compensatory or excessive hypertrophy in hypertensive heart. *Cardiovasc Res* 55: 76-82, 2002.
147. **Yankopoulos NA, Davis JO, Cotlove E, Trapasso M.** Mechanism of myocardial edema in dogs with chronic congestive heart failure. *Am J Physiol* 199: 603-608, 1960.
148. **Zanchi A, Stergiopulos N, Brunner HR, Hayoz D.** Differences in the mechanical properties of the rat carotid artery in vivo, in situ, and in vitro. *Hypertension* 32: 180-185, 1998.
149. **Zhang ZG, Chopp M, Goussev A, Lu D, Morris D, Tsang W, Powers C, Ho KL.** Cerebral microvascular obstruction by fibrin is associated with upregulation of PAI-1 acutely after onset of focal embolic ischemia in rats. *J Neurosci* 19: 10898-10907, 1999.

APPENDIX

Table 3-1: Distribution of subjects in experimental groups

	No Pulmonary Artery Banding	**Pulmonary Artery Banding**
Protocol 1 **Left Ventricular End-Diastolic Interstitial Fluid Pressure (P_{INT}) Volume (EVF) relationship**	**Group 1a** **Baseline**: 48 historic controls and 2 new controls for validation; (n = 50)	**Group 1b** **Control animals**: Left ventricle made chronically edematous (n = 3)
	Control animals: Left ventricle made acutely edematous by coronary sinus pressure elevation (n = 8)	**Chronically edematous**: Left ventricle made acutely edematous by coronary sinus pressure elevation (n = 5)
Protocol 2 **Left Ventricular Chamber Compliance**	**Group 2a** **Control animals**: Left ventricle made acutely edematous by coronary sinus pressure elevation (n = 5)	**Group 2b** **Chronically edematous**: Left ventricle made acutely edematous by coronary sinus pressure elevation (n = 3)

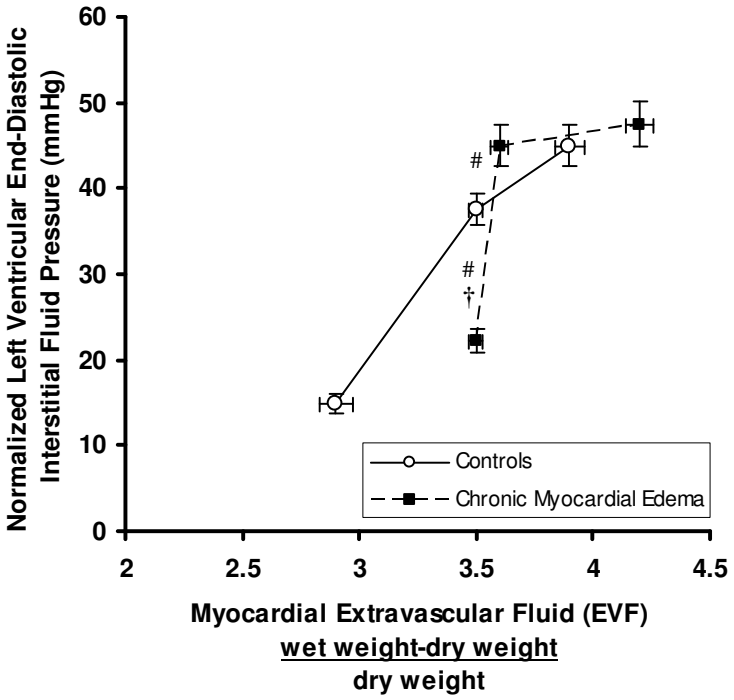

Figure 3-1: Normalized Left Ventricular End-Diastolic Interstitial Fluid Pressure plotted as a function of Myocardial Extravascular Fluid (EVF) [(wet weight-dry weight)/dry weight], indicating the degree of myocardial edema. The normalized value was calculated as the recorded myocardial left ventricular interstitial fluid pressure at end-diastole (P_{INT}) minus left ventricular end-diastolic chamber pressure. Open circles – controls made acutely edematous by coronary sinus pressure elevation. Solid squares – animals with chronic myocardial edema subjected to acute coronary sinus pressure elevation. Solid and dashed lines connect data points but are not regressions. (#) indicates statistically significant difference from group1a baseline animals. (†) indicates statistically significant difference from group1a control animals. Data plotted as mean $\pm$ SEM.

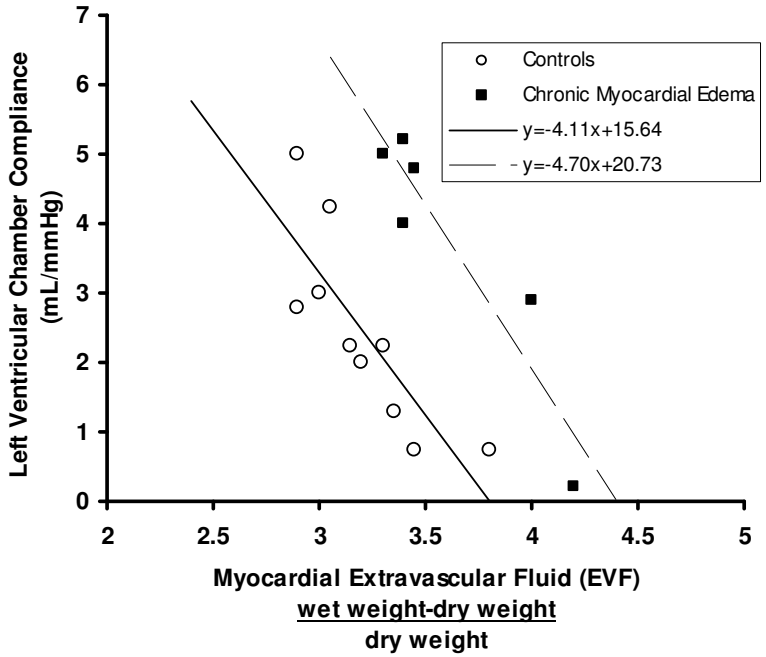

Figure 3-2: Left Ventricular Chamber Compliance plotted as a function of Myocardial Extravascular Fluid (EVF) [(wet weight-dry weight)/dry weight], indicating the degree of myocardial edema. Open circles – controls made acutely edematous. Solid squares – animals with chronic myocardial edema subjected to additional acute myocardial edema. Solid and dashed lines are regressions of control and chronic myocardial edema data respectively.

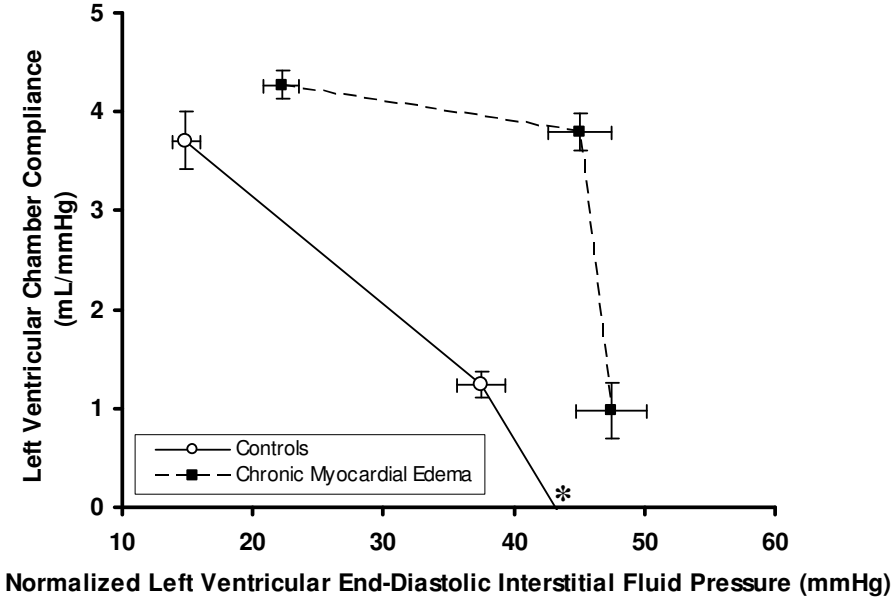

Figure 3-3: Left Ventricular Chamber Compliance plotted as a function of Normalized Left Ventricular End-Diastolic Interstitial Fluid Pressure. The normalized value was calculated as the recorded myocardial left ventricular interstitial fluid pressure at end-diastole (P_{INT}) minus left ventricular end-diastolic chamber pressure. Left ventricular chamber compliance values were obtained by substituting myocardial extravascular fluid values from Fig. 3-1 into regression equations from Fig. 3-2. Error bars for left ventricular chamber compliance were also computed from regression equations. We placed boundary limits on the lower values of EVF to avoid negative or non-physiological values of left ventricular chamber compliance (*). Solid and dashed lines connect data points but are not regressions. Open circles – controls made acutely edematous. Solid squares – animals with chronic myocardial edema subjected to additional acute myocardial edema. Data plotted as mean $\pm$ SEM.

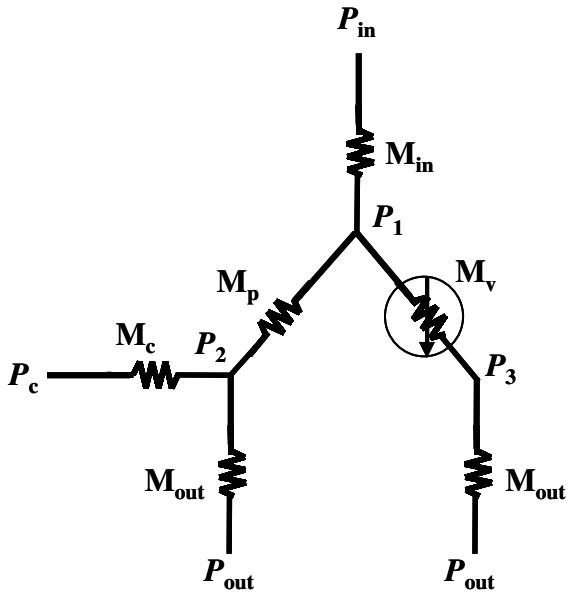

Figure 4-1: Schematic of a portion of a microvascular network expressed in terms of an electrical equivalent used for mathematical modeling. P_{in} and P_{out} are the input and output pressures, respectively; P_1, P_2, and P_3 were the intermediate pressures. P_c was the input pressure for the collateral. M_{in} is the upstream arteriole, M_p is the parallel arteriole, M_c is the collateral arteriole, M_{out} is the lumped downstream network, and M_v is the vessel of interest (denoted by the circle). M_v has a variable resistance.

Figure 4-2: Enhanced image of a Pallid bat wing acquired using a flat bed scanner illustrating several arterial bifurcations. B_{in} is the upstream arteriole, B_p is the parallel arteriole, B_c is the collateral arteriole, B_{out} is the entrance to the downstream network and B_v is the vessel of interest (circle). The arrows represent the direction of blood flow.

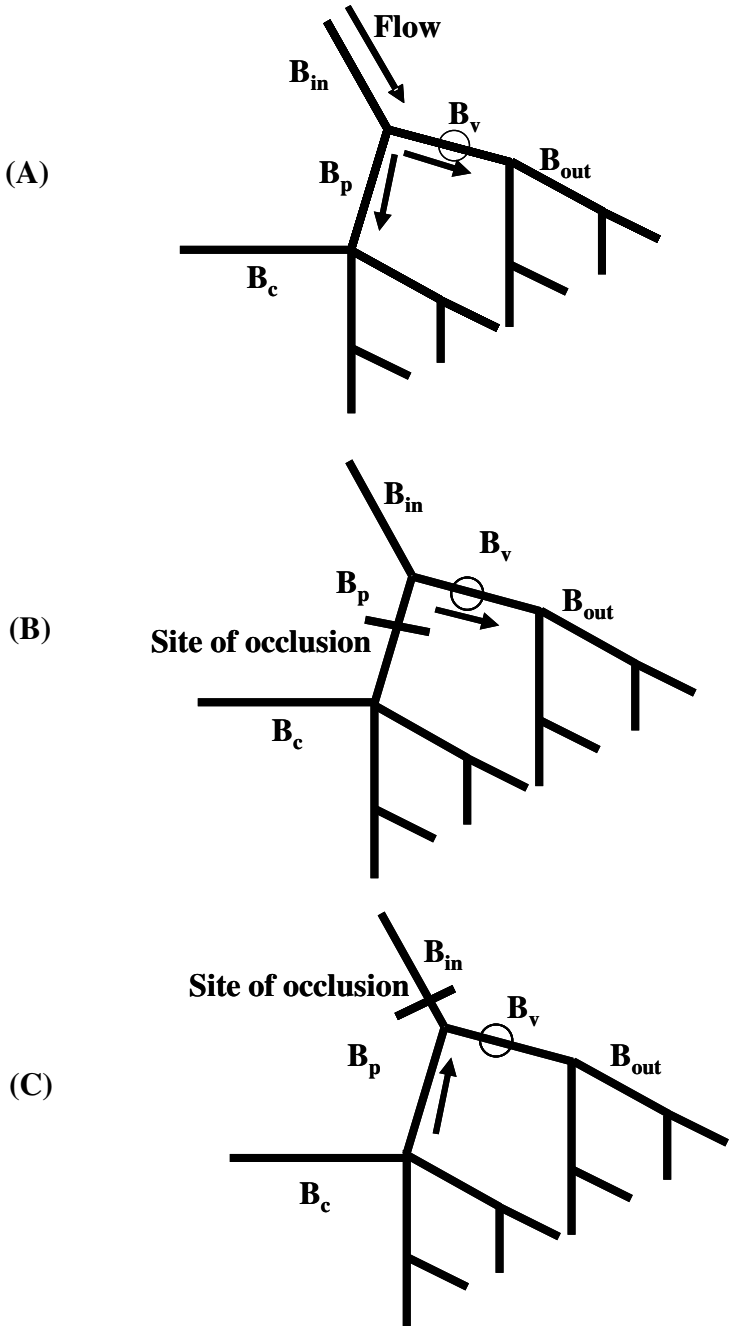

Figure 4-3: (A) Schematic of the bat wing with (B) occlusion of parallel arteriole B_p and (C) occlusion of upstream arteriole B_{in}. The arrows represent the direction of blood flow, the circle represents the vessel of interest (B_v) and the solid line represents the site of occlusion.

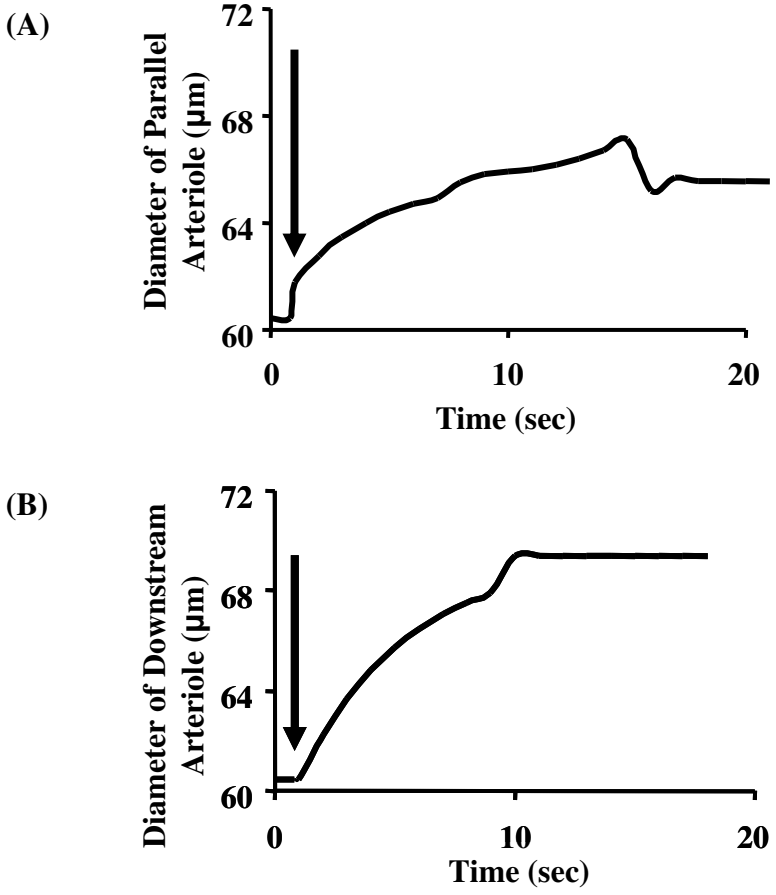

Figure 4-4: Model results representing the transient changes in diameter of vessel of interest (M_V) with complete occlusion (100%) of (A) parallel arteriole M_p and (B) upstream arteriole M_{in} plotted as a function of time. Arrows indicate arteriolar occlusion.

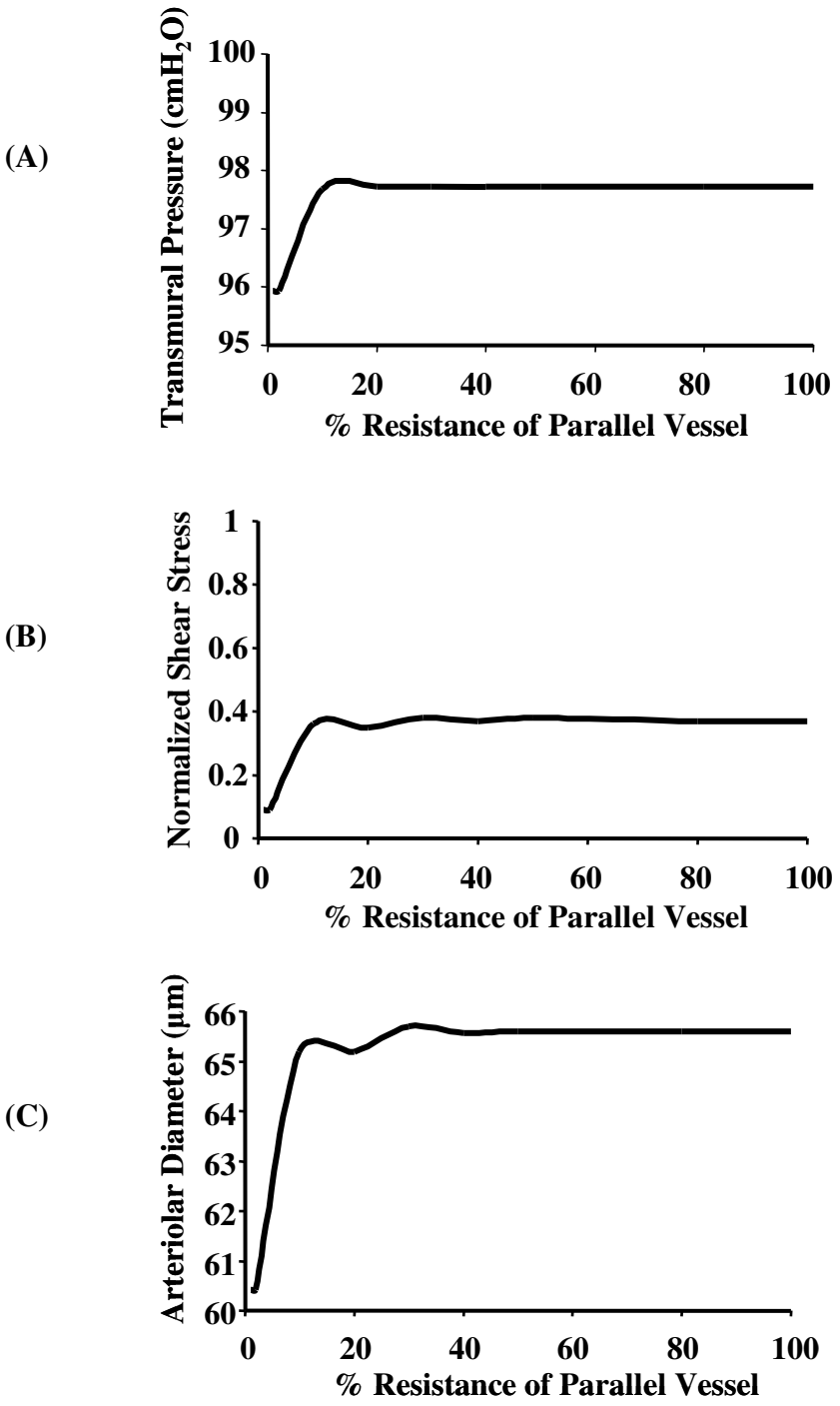

Figure 4-5: Model results representing the changes in steady state values of (A) normalized endothelial shear stress, (B) transmural pressure and (C) diameter of vessel of interest M_V plotted as a function of progressively increasing resistance of parallel arteriole M_p from 0% to 100%.

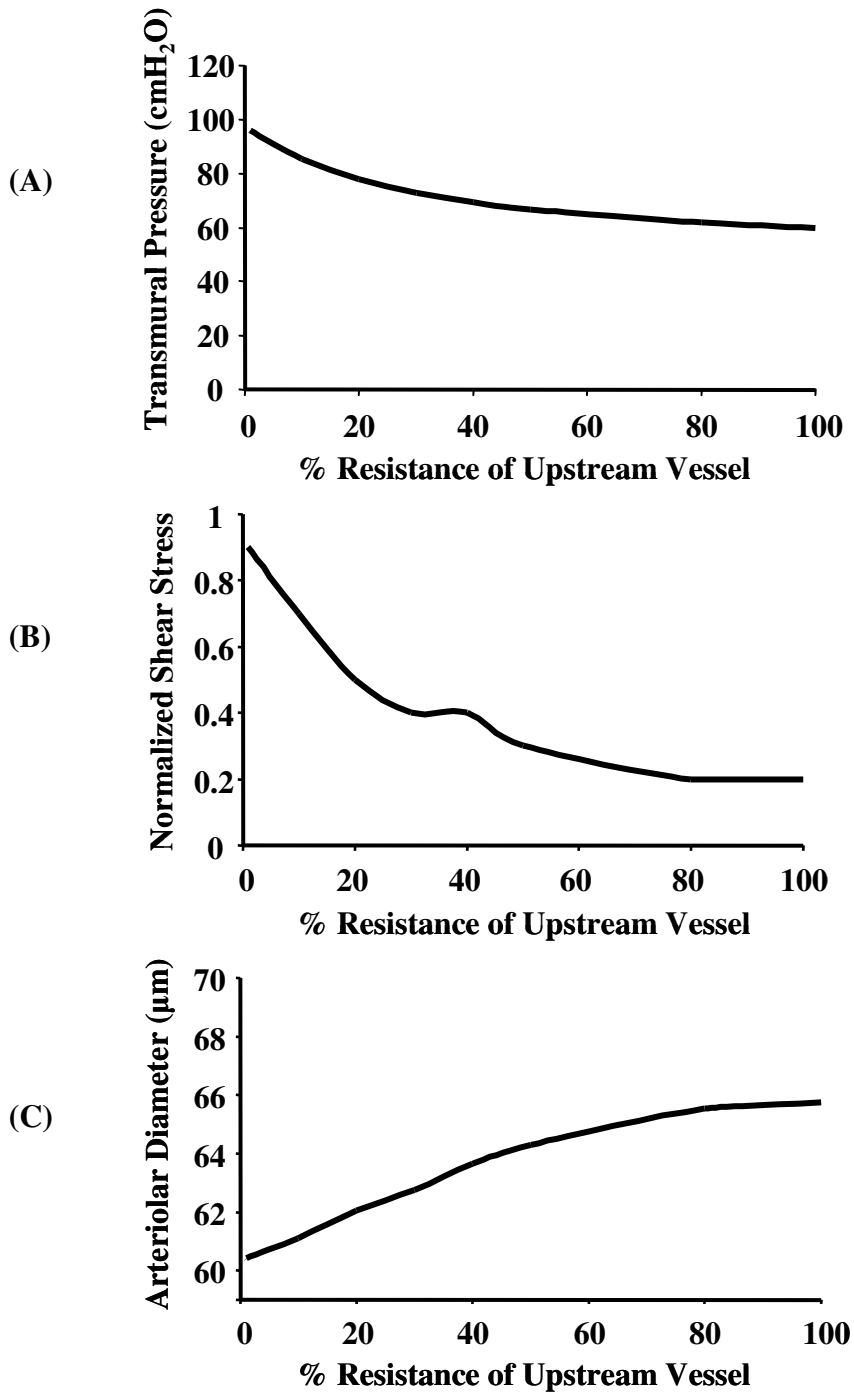

Figure 4-6: Model results representing the changes in steady state values of (A) normalized endothelial shear stress, (B) transmural pressure and (C) diameter of vessel of interest M_V plotted as a function of progressively increasing resistance of upstream arteriole M_{in} from 0% to 100%.

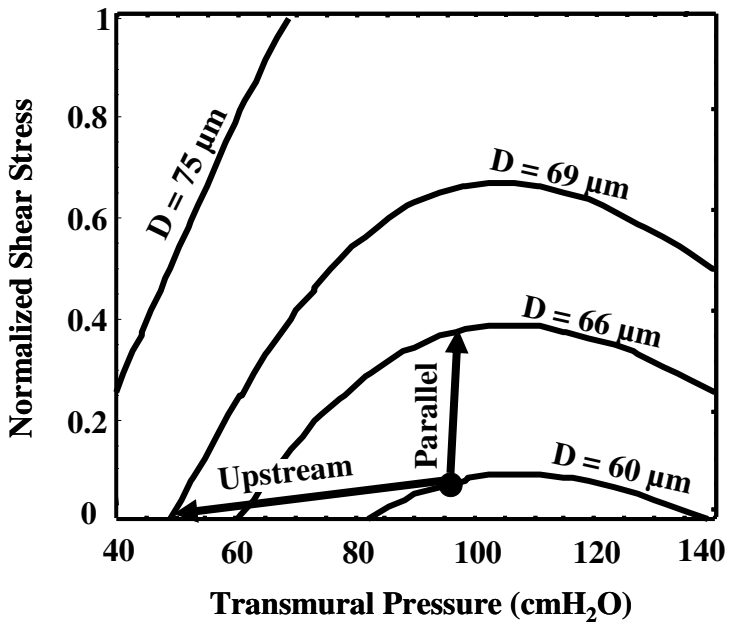

Figure 4-7: Contour plot representing changes in arteriolar diameter (D) is plotted as a function of transmural pressure and normalized shear stress in the mathematical model portrayed in Fig. 4-1. Solid circle represents the initial steady-state value of vessel of interest M_V. Arrows represent adaptation of vessel to new steady state values after parallel and upstream occlusion protocols.

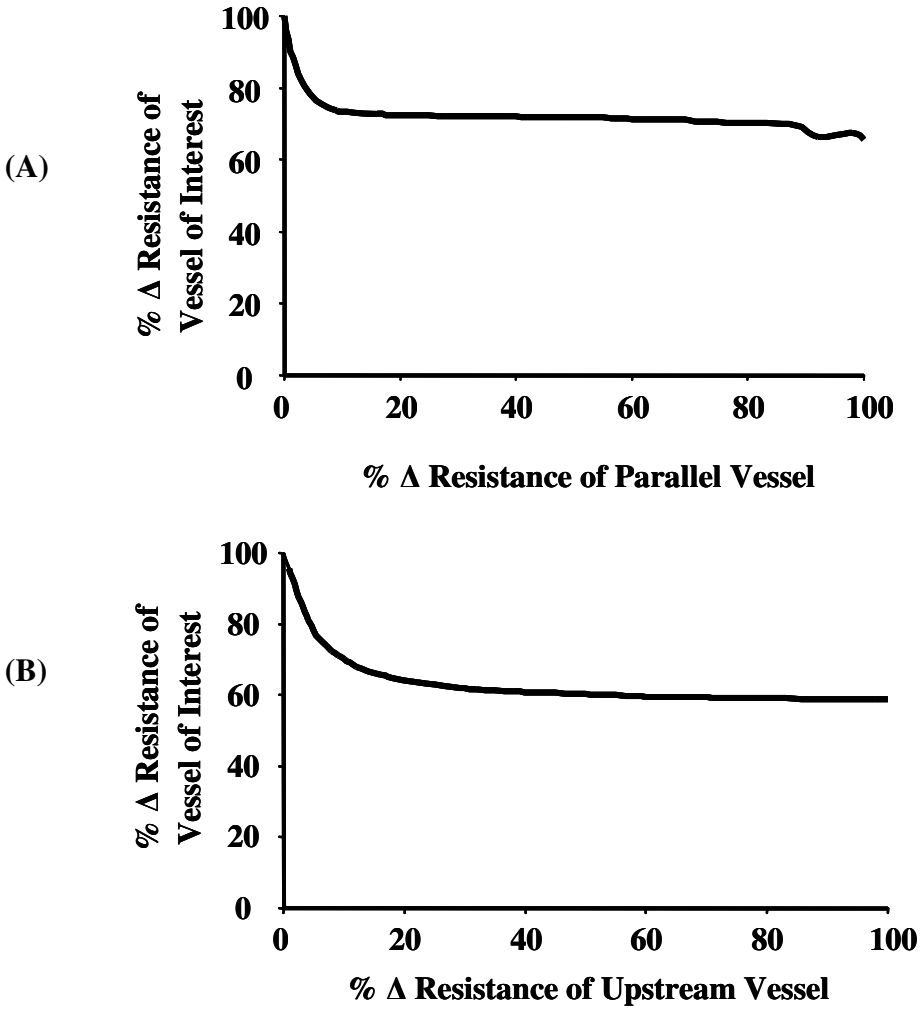

Figure 4-8: Model results illustrating the decrease in resistance of vessel of interest M_v when a parallel arteriole M_p or upstream arteriole M_{in} is progressively occluded.

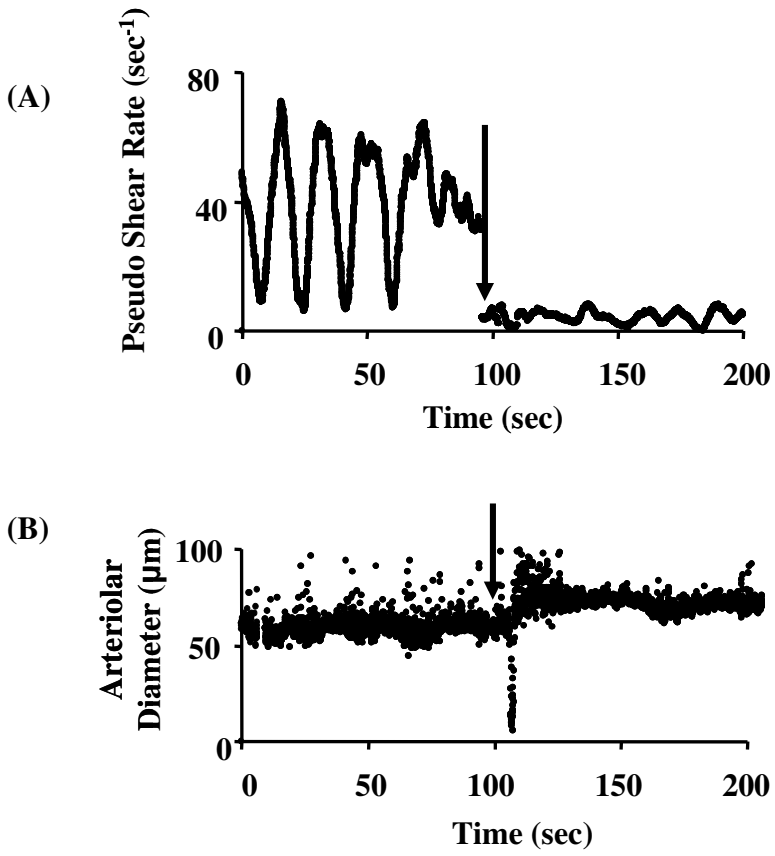

Figure 4-9: Real-time pseudo shear rate and arteriolar diameter when an upstream arteriole (B_{in}) is occluded as shown in Fig. 4-8. Data recorded for 100 seconds before and during occlusion. Arrows indicate arteriolar occlusion. The automated diameter tracker was reset at the time of occlusion.

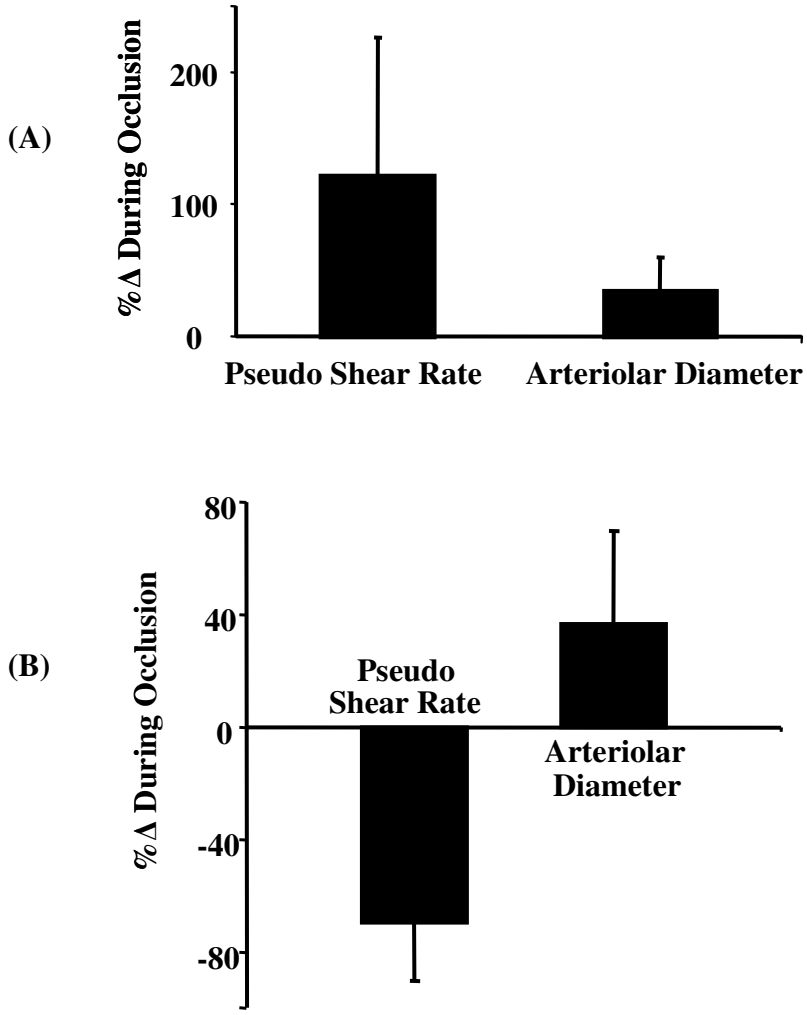

Figure 4-10: (A) Percentage change of pseudo shear rate and arteriolar diameter plotted $\pm$ SD (n=4 bats and 7 vessels) when a parallel arteriole B_p was occluded for 2 minutes, as illustrated in Fig. 4-3B. (B) Percentage change of arteriolar diameter and pseudo shear rate plotted $\pm$ SD (n=8 bats and 26 vessels) when an upstream arteriole B_{in} was occluded for 2 minutes, as illustrated in Fig. 4-3C.

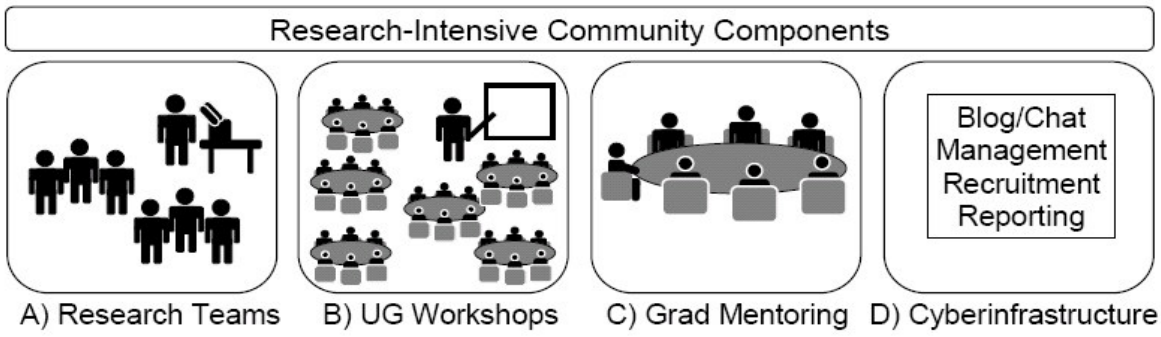

Figure 5-1: Components of the Research-Intensive Community model developed at Texas A&M University. A) Research teams consisting of three undergraduate students mentored by a "team leader", B) Undergraduate workshops managed by lab director, C) Graduate Leadership Forum and D) computer-mediated communication.

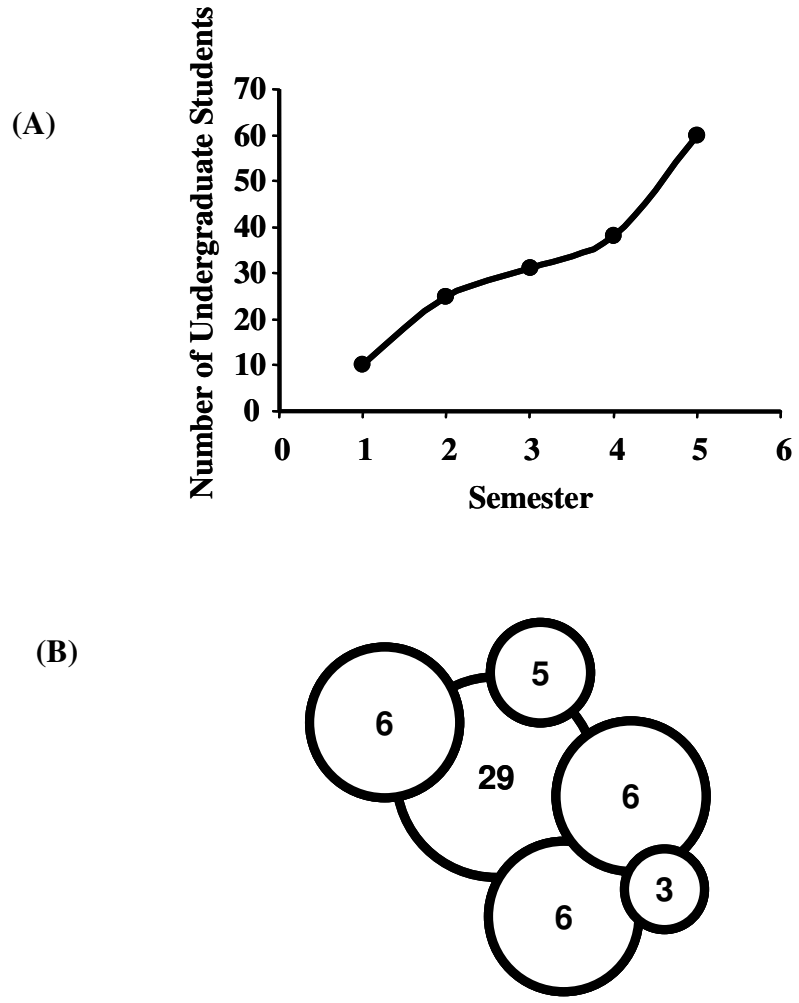

Figure 5-2: A) Number of undergraduate students participating in the Research-Intensive Community each semester from summer 2004 to spring 2006. B) Graphical representation of interlocking affinity groups in fall 2006. Each affinity group (circles) consisted of one or more teams mentored by a faculty member that shared particularly close project goals. Numbers represents undergraduates in each group.

Table 5-1: The numbers for undergraduate students, graduate students, and faculty participating in the Research-Intensive Community per semester. Because some undergraduate students continued for more than one semester, the numbers do not represent a total number of students in the program.

	Summer 04	Fall 04	Spring 05	Fall 05	Spring 06
Undergraduates	10	25	31	36	60
Graduate students	10	4	6	6	11
Faculty	2	1	2	2	5

Table 5-2: Goals of undergraduate students as part of the Research-Intensive Community.

	Self-Interest	*Collective Interest*
Educational Practice	▪ Develop research experience and substantive products for resume ▪ Discover if a research career might be a personally satisfying choice ▪ Experience alternative approaches to research apprenticeship ▪ Increase familiarity with a basic science subject area ▪ Increase personal capacity for productive output in preparation for graduate school ▪ Learn more about research careers to inform immediate academic decisions ▪ Seek academic guidance for pursuing a research career	
Research Practice	▪ Apply formal knowledge to research problems ▪ Become acquainted with the research aspect of the medical profession ▪ Become acquainted with the research process ▪ Gain experience in a professional work environment ▪ Gain knowledge about how to publish research ▪ Increase personal capacity for critical problem solving ▪ Network and establish relationships with research professional ▪ Satisfy personal curiosity about the social experience of a conference ▪ Satisfy personal curiosity about how bodily systems work ▪ Uncover whether research could be applied to health issues	

Table 5-3: Goals of team leaders as part of the Research-Intensive Community

	Self-Interest	*Collective Interest*
Educational Practice	▪ Conduct unique research to broaden experience and improve curriculum vita ▪ Becoming a skilled and knowledgeable researcher in multi-disciplinary setting ▪ Collecting data and writing manuscripts for graduation ▪ Course credit for program of study ▪ Desire to be informed about health issues ▪ Develop leadership skills to manage multi-disciplinary research teams ▪ Learn what is required to maintain a faculty position within a research institution ▪ Seeking more affective, sensate learning experiences than traditional academic coursework	▪ Helping UG co-author conference abstracts and improve their resumes ▪ Helping UG co-author conference abstracts and improve their resumes ▪ Helping UG gain skills to participate in research communities (socialization) ▪ Mentoring UG through the research process
Research Practice	▪ Personal pursuit of discovering knowledge about the unknown ▪ Publishing manuscripts and conference abstracts ▪ Seeking to satisfy intellectual curiosity	▪ Answering questions and defending knowledge claims to a scientific community ▪ Conduct research that will improve the lives of others ▪ Help principal investigator with tenure and funding ▪ Helping UG develop their research interests and projects ▪ Increase productivity and improve profile of research group ▪ Leading UG teams to get laboratory work done for projects

VITA

Name:	Ketaki Vimalchandra Desai
Address:	MS 4466, Room# 300A Dept. of Physiology and Pharmacology College of Veterinary Medicine Texas A&M University, College Station, TX 77843-4466
Email Address:	ketaki.desai@gmail.com
Education:	B.S., Mechanical Engineering, Pune University Pune, India, 2002 Ph.D., Biomedical Sciences, Texas A&M University College Station, TX, 2008
Training:	Graduate Research Assistant, Cardiovascular Systems Dynamics Laboratory, Texas A&M University, 2003-2007 Graduate Teaching Assistant, Department of Physiology and Pharmacology, Texas A&M University, 2005-2007 Graduate Assistant Non-Teaching, Engineering Academics Programs Office, Texas A&M University, 2002-2003